Utrecht University

Msc. Research
GEO4-1520

Effect of climate change and human perturbation on groundwater-streamflow interactions: recent and projected trends for North-America

Author

Sophie De Kock (6265944)

1st Supervisor

Dr. Rens van Beek

2nd Supervisor

Prof. Dr. Marc Bierkens

30 ECTS

2018 - 2019

Universiteit Utrecht

Contents

Abstract

Groundwater is a very important natural resource as it is the main source of freshwater. Although this resource is depleting over the world because of increasing water demands mainly due to irrigation (Aeschbach-Hertig and Gleeson , 2012). Recharge of groundwater is highly dependant on climate and on human water use. The main objectives of this research are to point out the areas in North-America that are becoming wetter and drier, and to assess if these changes are mainly due to human or climate influence. Knowing where humans have the most influence on stream interaction changes, enables us to determine which areas we should dedicate more attention and what kind of management policy should be applied there. The streams were classified into gaining, losing, intermittently disconnected and continuously disconnected. The projections of groundwater-streamflow interaction changes only take into account climate changes. These projections are run under RCP 8.5 according to three different GCMs that represent a dry, average and wet scenario. These three GCMs were used in order to know what is the probability range of groundwater-streamflow interaction change in the future. In order to make this analysis possible we used data previously simulated with PCR-GLOBWB (Beek (van) and Bierkens , 2009) that is a physically based hydrological model at high spatio-temporal resolution that was coupled with MODFLOW (Harbaugh et al. , 2000) in order to simulate groundwater and surface water interactions.

The first step of this research was to validate the simulated surface water discharge and groundwater level from PCR-GLOBWB against observed data from USGS. Then, the groundwater-streamflow interaction on the past period could be analysed and compared for a natural run and runs that takes into account human and climate influence for different forcing data. After that, an analysis and a quantitative as well as qualitative comparison of the three future scenarios were produced. A small analysis of changes in groundwater-streamflow interactions over the world for the period 1901-2010 was realised in order to have a slight insight on what is happening worldwide. Maps showing where the changes happened were created for each run and an analysis on stream order influences on these changes was performed.

As expected we show that changes are more likely to happen at the transition between a wet and a dry area. The analysis on the historic period shows that streams located in the north of the US great plains become drier as well as the Missouri River and the border between Guatemala and Mexico. There is some variation according to the set of forcing data used. The rate of increase in gaining streams is lower for the Natural run than for the Non-natural runs still the Natural run is the run with the most gaining streams. The Natural run also shows the sharpest decrease as well as the smallest amount in continuously disconnected streams. Our main finding is that the influence of climate change has more impact on the groundwater-streamflow interaction than human influence. According to two GCMs out of three, North-America is more likely to become wetter than drier, although the third GCM tends strongly toward a drier trend. The analysis on stream orders shows that they do not act all similarly for two out of three runs of the historic period but do for the projection runs.

As the historic scenarios and projection scenarios were not run using the same set of forcing data, they could not be compared with each other. In order to remedy this problem a new run was made covering the historic and future period and using one of the GCM used previously calibrated with historic data as forcing data. For a question of time restrictions, this run was not run using exactly the same North-America mask as the previous runs. This run shows an evolution toward drier stream states. The areas of change in this run are different from the ones in the others run. Indeed it shows that the wetter streams are located on a small area in the north of the US Great Plains and the drier streams are on the Great Plains area, around the border between the Great Plains and the Intermountain Plateau. It shows also that the seasonal behaviour of groundwater-streamflow interaction is changing.

1 Introduction

1.1 Background

Groundwater represents 30% of the fresh water resources, it is used for domestic, agricultural and industrial purposes. Natural groundwater recharge occurs via precipitation and leakage intrusion from streams (Taylor et al. , 2013). Recharge of groundwater also occurs via return flow from crop irrigation. Therefore, it is highly dependant on climate, land cover and underlying geology (Taylor et al. , 2013). Recent climate changes have led to increasing variability in precipitation, soil moisture and surface water which all play a role in groundwater recharge.

In this thesis, the changes in interaction between surface water and groundwater will be analysed mostly for the US and North-America in general. As at the interaction between groundwater and surface water, there is no distinction between these two sources of water, groundwater-surface water interactions will be referred to as groundwater-streamflow interaction. There are three different modes of interaction between groundwater and streamflow. These modes are: gaining stream, losing stream connected to groundwater and losing stream disconnected from groundwater (Figure 1). In a gaining stream, the river is recharged by groundwater flow because the groundwater head is above the river head whereas in a losing stream the river recharges the groundwater flow because the river head is above the groundwater head. When groundwater gets disconnected from the stream, the infiltration from the river reaches a maximum and so it is not dependent on the groundwater level anymore (Figure 2). This infiltration of water from the river stream is called "reduced stream flow" in figure 2, but it is more commonly called "stream capture" or "stream depletion". Stream capture is defined as the reduction in streamflow to supply pumping (Konikow and Leake , 2014). Due to pumping of water, a gaining stream can be turned into a losing stream and if the pumping rate is too high the groundwater table can drop below the stream bed and this is the beginning of groundwater depletion. Even within a single catchment, it is possible to find the three different modes of interaction between surface water and groundwater. This is because it varies over space depending upon topography, lithology and it varies over time, both within a year depending upon the amount of precipitation and evaporation and also from year to year depending upon whether it is a dry or a wet year and due to the effects of climate change.

As the world population is growing, water demand is increasing, leading to pressure on water supply. Climate change has an effect of making arid and semi-arid regions even drier (Taylor et al. , 2013). The economic development allows those countries suffering from a lack of fresh surface water to pump groundwater deeper and deeper from the ground which can lead to a disconnection between the groundwater and the streamflow or/and to an increasing groundwater storage depletion. It is already known that groundwater storage is depleting in many regions over the world (Aeschbach-Hertig and Gleeson , 2012). The consequences of groundwater depletion can be an increase in food price due to an increase in the cost of groundwater pumping, it can also lead to subsidence of land and so affect infrastructure (Bartolino and Cunningham , 2003), lower discharge from groundwater to stream has an impact on the ecosystem (Graaf (de) et al.,submitted) due to the specific composition of groundwater but also due to the level of water.

Studies have already been made in order to assess the impact of an overuse of nonrenewable groundwater (Dhungel and Fiedler , 2016) and globally assess the contribution of nonsustainable groundwater to irrigation in order to know which areas over the world are at risk (Wada et al. , 2012). De Graaf et al. (submitted) assessed where and when environmentally critical streamflow, required to maintain healthy ecosystems, will no longer be sustained due to groundwater pumping. In the same article they mapped the cumulative groundwater depletion over the world and made predictions until the year 2100. Konikow (2015) evaluates long-term changes in groundwater storage in the United States for 1900–2008. In this paper he assess the rate and the intensity of groundwater depletion in the United States and gives explanations for apparent recovery or increased depletion of groundwater storage. The focus of this current research is not on groundwater depletion but on the evolution of groundwater-streamflow interaction over years that might lead to groundwater depletion if groundwater becomes permanently disconnected from the streamflow.

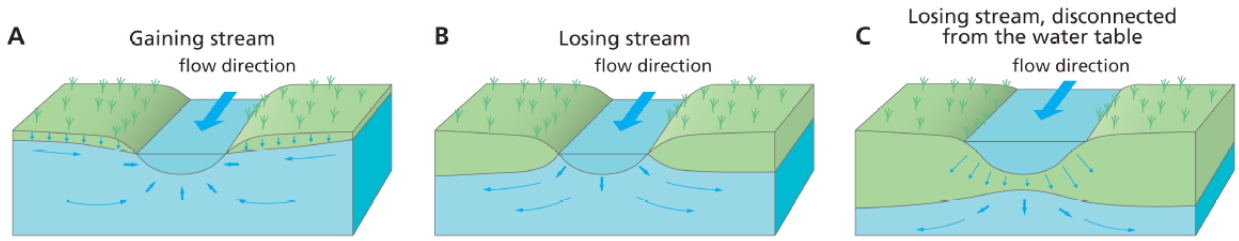

Figure 1: Groundwater-streamflow interaction (Graaf (de) et al.,submitted): A: gaining stream; B: losing stream; C: losing stream disconnected from the groundwater table.

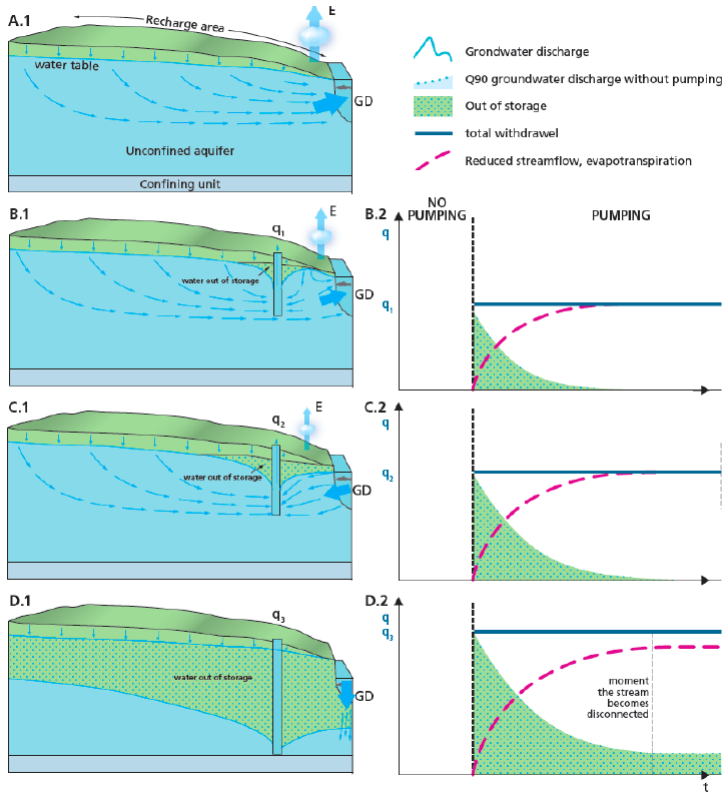

Figure 2: Groundwater-streamflow interaction (Graaf (de) et al.,submitted): A) Gaining stream, natural conditions; B) Gaining stream,limited pumping ; C) Connected losing stream, higher pumping rates ; D) Disconnected losing stream, more intense groundwater pumping rates. Column 1) cross section of the stream and surrounding groundwater; 2) graph displaying the total withdrawal, reduced streamflow, evapotranspiration and the portion out of storage.

1.2 Problem definition

It is from groundwater resources that most of the fresh water we use comes from. It is expected that in the future the water demand will increase and that surface water will not be enough to handle this increase. Therefore, an increase in groundwater extraction will follow which would lead to more streams going from gaining to losing and from losing to disconnected, until they become continuously disconnected and lead to groundwater depletion. Having a better knowledge on how groundwater interacts with streamflow is thus important because groundwater recharge depends partly on surface water. To know where streams are becoming drier but also where they are becoming wetter is valuable information for determining a better protection strategy and therefore mitigate the groundwater depletion problem. However, fluxes between groundwater and surface water are difficult to assess as it is highly variable depending on geology of the subsurface, land use and climate. Also, aquifer and streams exchange water horizontally and vertically which means that it is a three-dimensional process and most hydrologic modelling studies have used one- or two-dimensional models. (Sophocleous , 2002). In this research the three-dimensional hydrologic model PCR-GLOBWB (Beek (van) and Bierkens , 2009) coupled with MODFLOW (Harbaugh et al. , 2000) was used in order to simulate lateral groundwater flow and fluxes between surface water and groundwater. However, it does not account for the stream capture phenomena (see section 1.1) which can lead to an overestimation of groundwater storage depletion (Konikow and Leake , 2014).

The objectives of this research is to show where the streams become wetter and drier, mainly in North-America but also for the world. A quantitative assessment of human and climate change influences on the evolution of stream state in North-America is given. Knowing where humans have a significant impact on stream states allow to focus our attention on vulnerable areas where policy can be changed, and accurate protection strategy can be identified and applied. The changes in stream states will be also analysed quantitatively and qualitatively for three different future scenarios under the 8.5 representative concentration pathway (RCP). The 8.5 RCP assumes a radiative forcing value which is a cumulative measure of human emissions of greenhouse gas, in the year 2100, of 8.5 W/m^2. This RCP was chosen because it is the worst case scenario it is thus the one that will show the biggest changes and also it is better to be prepared for the worst. These three scenarios only take into account climate changes but not a growing human influence as they assume a constant water demand over time. Again this may allow us to devise a suitable management approach that may mitigate human vulnerability to climate change and guarantee more sustainable groundwater extraction and promote food security. In this research, the influences of climate change were analysed but not the influences of socio-economic changes because it was assumed that climate change would have greater impact than socio-economic changes.

This thesis is primarily based on hypotheses and simulation data, it is one of the reasons for which we start with a validation of the simulated data from the model by comparing them with observed data. The research questions answered in this thesis are:

- According to a single catchment, how the model performs compared to observations with respect to observed piezometric level and discharge?
- How the surface water and groundwater interaction has evolved from 1901 to 2010 in North America and the world? What could be the reason of theses changes?
- Comparing natural historic run and non-natural historic run, where in North-America can human impact be seen the most and at which extent (from 1960 to 2004)?
- How the surface water and groundwater interaction will have evolved in North-America from now to the end of this century according to three different GCM's?
- What is the range of uncertainty when comparing the result from the 3 different GCM runs? What are the differences between the worst and the best scenario? Which of them seem the most suitable?

2 Method

2.1 Groundwater-streamflow interaction

In order to know if a stream is gaining or losing, a comparison between the river and the groundwater head is necessary. Indeed as explained in section 1.1, if the river is lower than the groundwater head the stream is considered as gaining because in this case the groundwater travels up and fills the stream. This is due to the fact that the water goes from high potential to low potential. If the river head is higher than the groundwater head the stream is losing. This means that the surface water infiltrates the ground until reaching the groundwater table. A losing stream can be connected or disconnected from the groundwater table depending on if it is connected to the stream via a saturated zone (Fig.1B) or via an unsaturated zone (Fig.1C). Figure 2 shows what are the impacts of pumping water from groundwater that is discharging in a stream. It shows that with a low pumping rate only groundwater is intercepted by the well (Fig.2B) and groundwater is still discharging in the stream so the stream is still a gaining stream. After a period of time the system will find a new balance and groundwater storage will stop depleting, only the amount of water available for evapotranspiration decreases. If the pumping rate increases slightly (Fig.2C) groundwater and the water from the stream are intercepted by the well, changing the gaining stream into a losing stream still connected to the groundwater table. The water available for evapotranspiration is not enough to reach a new equilibrium and therefore water from the stream gets intercepted by the well too. If the pumping rate increases even more (Fig.2C), water from the stream is not sufficient to handle the increasing demand of water, as a consequence a new equilibrium is never reached and groundwater storage continues depleting.

2.2 The model

The PCR-GLOWB (PCRaster Global Water Balance) (Beek (van) and Bierkens , 2009) model used for this research was a development version of PCR-GLOBWB2 explained in detail by Sutanudjaja et. al (2018). PCR-GLOBWB2 is a grid-based global hydrology and water resources model with a spatial resolution of 5 arcmin in latitude and longitude and a daily time resolution. Human water use is taken into account by estimating water demands for irrigation, livestock, industry and households and subtracting it from groundwater, surface water, desalinated water based on availability and global datasets about global groundwater and surface water withdrawal. Return flow and water consumption are included in water availability. For this study, PCR-GLOBWB (Beek (van) and Bierkens , 2009) was coupled with MODFLOW (Harbaugh et al. , 2000) in order to simulate lateral groundwater flow and fluxes between surface water and groundwater but it does not account for the stream capture phenomena. The surface water routing used was a simple accumulation of the fluxes, it is the less complex choice of routing in PCR-GLOBWB but it was the one with the least computational time.

2.3 Data explanations

Table 1: Characteristics of the seven runs analysed in this thesis

Summary of the different runs					
Period	**Name**	**Mask**	**Years**	**Forcing**	**Data from**
Historic	Natural Inge	North-America	1960-2004	- CRU 3.21 ERA 40 - ERA-Interim	Inge de Graaf
	Non-Natural Inge	North-America	1960-2010	- CRU 3.21 ERA 40 - ERA-Interim	Inge de Graaf
	Non-Natural Edwin	North-America / World	1901-2010	CRU 3.23 ERA-20C	Edwin Sutanudjaja
Historic + Future	Reference	US	1950-2099	GCM HadGEM	Edwin Sutanudjaja
Future	HadGEM	North-America	2010-2100	GCM HadGEM	Inge de Graaf
	GFDL	North-America	2010-2099	GCM GFDL	Inge de Graaf
	MIROC	North-America	2010-2099	GCM MIROC	Inge de Graaf

In order to compare the groundwater head with the river head, the data from Edwin sutanudjaja and Inge de Graaf that they computed for other studies, were used. This data were computed for the entire world at a resolution of 5 arcmin. Table 1 shows which runs belong to Inge and which ones belong to Edwin and what are their main characteristics. For the runs from Edwin the data, previously computed, are the surface water storage in meters, the groundwater head in meters, the fraction of surface water on a cell and the river bed elevation in meters.

From Inge, the same data was available except for the fraction of surface water, that was thus estimated. An equation that linked discharge to dynamic fraction of water was computed using the data from the non-natural run of Edwin Sutanudjaja (figure 3) for North-America. The lake (and reservoir, if not the natural run) areas had to be corrected by using a mask for the lake (and reservoirs) and considering their dynamic water fraction constant over time. The mask of lake and reservoir areas is shown in the appendix on figure A.1. Using this method for the non-natural run of Edwin Sutanudjaja and comparing the results of the estimate dynamic water fraction with the simulated one, gave us a root mean square error (RMSE) of 0.0808. The estimated river head compared with the model one, gave us a RMSE of 0.565. These RMSE were considered as low enough to apply this method in order to compute the dynamic water fraction. Figure 3 shows the graph relating discharge with dynamic fraction of water only for one cell, it changes for every cell. This cell was situated on the Mississippi River, this was chosen because this river has a lot of discharge and shows seasonal variations.

To distinguish a gaining and a losing stream, the river head and groundwater head have to be compared. In order to make them comparable, the river head and the groundwater head from the river bottom were computed. The groundwater head in meters from the river bottom was computed by subtracting the river bed elevation from the groundwater head elevation. For having the river head with respect to the river bottom, the surface water storage was divided by the fraction of surface water on a cell. Sometimes the surface water storage value appears as negative, to avoid that, we set zero as the minimum value. In this study we assumed that for the stream to be disconnected from the groundwater, the groundwater head has to be 1 meter below the river bottom and to be continuously disconnected, the stream has to be disconnected for at least two years in a row. Inge de Graaf in her paper (Graaf (de) et al.,submitted) showed with a sensitivity analysis that 2 years in a row is a good choice because there is a great difference between choosing 1 year or 2 years but there is almost no difference between 2 and 5 years. In her paper, Inge was analysing when we can consider that the stream flow is affected by groundwater pumping.

On table 1, it is shown that the historic runs from Edwin and from Inge do not have the same meteorological forcing data. Inge de Graaf used CRU 3.21 ERA-40 (Uppala et al. , 2005) for the period 1960 to 1979 and ERA-Interim (Dee et al. , 2011) for the period 1979 to 2010 whereas Edwin Sutanudjadja used CRU 3.23 ERA-20C (Poli et al. , 2016) for the period 1901 to 2010. ERA-40 is the least accurate of the three forcing data-sets cited, it is the predecessor of ERA-interim for which the period starts in 1979. The main difference between ERA-Interim and ERA-20C is the time period that is 1979 to current time and 1901 to 2010 respectively as well as the horizontal resolution which is 80 km and 125 km respectively. According to Poli et. al (2016 and 2013) ERA-20C gives a better result for precipitation minus evaporation and for the total column water vapor and the temperature trends in ERA-20C differ from those of ERA-Interim with ERA-20C showing a greater global warming than ERA-Interim.

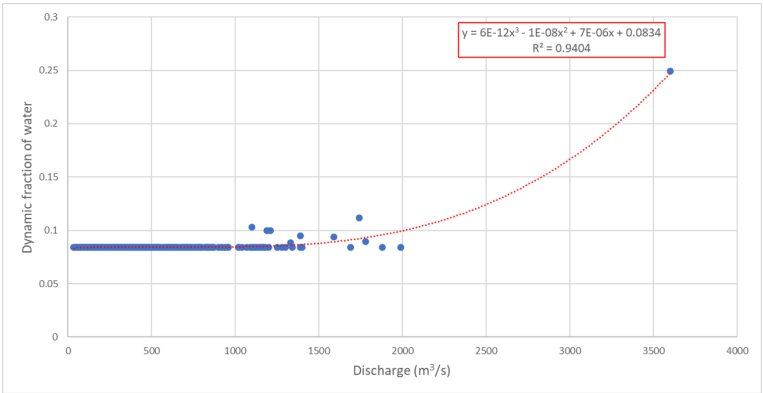

Figure 3: Correlation plot between discharge and dynamic fraction of water according to the historic non-natural run of Edwin for North-America. The equation that linked these two parameters and the determination coefficient are both displayed on this figure

.

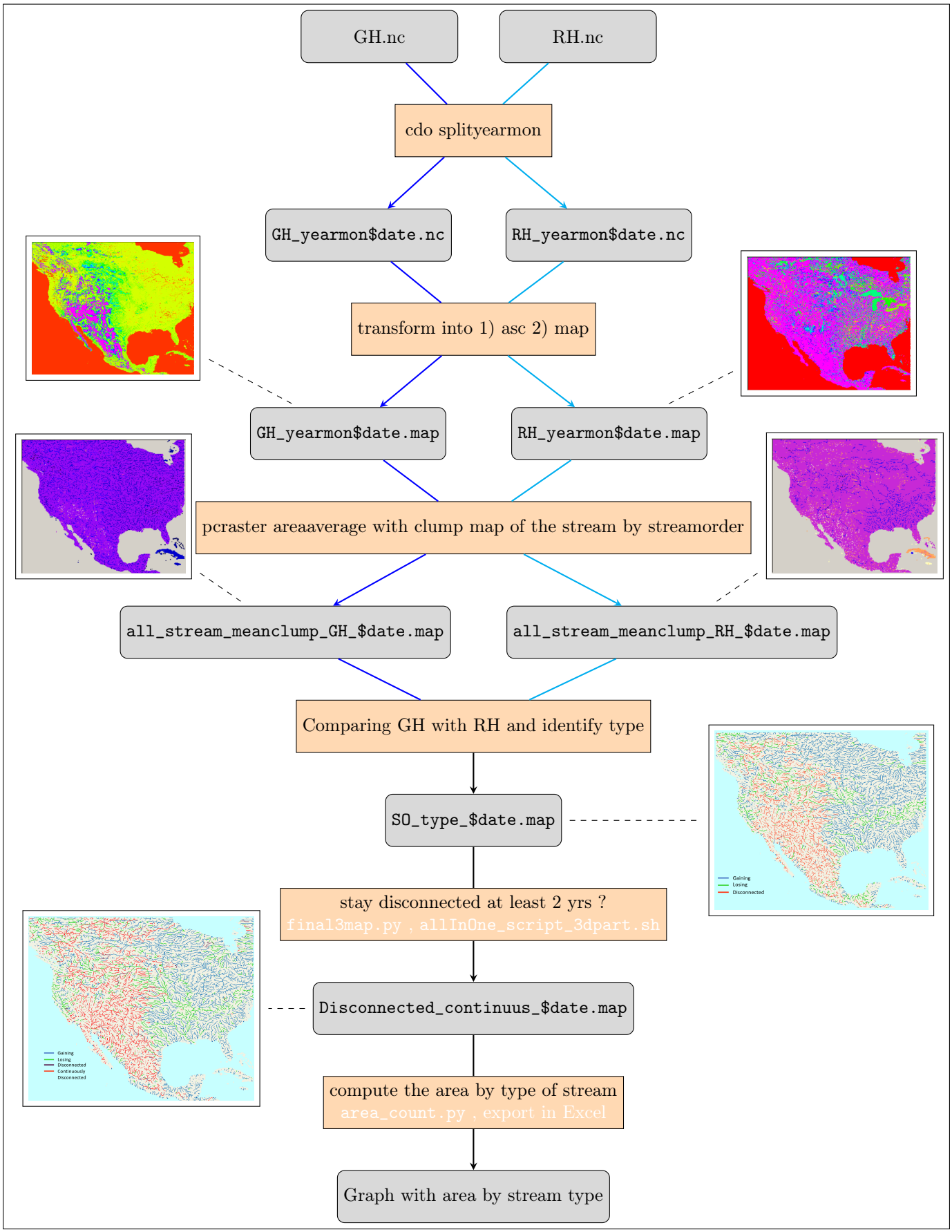

Figure 4: Method applied in order to make the graphs and maps presented in this study, GH stands for groundwater head and RH for river head. Grey boxes : are the results (maps, graps). Orange boxes : are the process which lead to the results. White comments : name of the script used (available in the appendices section D)

2.4 Runs description

The seven runs analysed in this study are displayed on table 1. There are three historic runs in which there are two non-natural runs and one natural run. The non-natural run from Edwin is run from 1901 to 2010 and is considered to give a more accurate result due to Edwin's choice of meteorological forcing data (Poli et al. , 2013, Poli et al. , 2016). However, analysing the non-natural run from Inge (1960-2010) is still important because it used the same forcing data set as for the natural run (1960-2004) from Inge, which makes them more comparable between each other. The comparison between the natural and non-natural runs is useful for determining the extent of climate change influence and human influence on the changes of stream states over time. The comparison will allow us to know where the human impacts are the strongest in North-America.

There are three runs for the future, each of them are run using a different General Circulation Model (GCM) under RCP 8.5. These three GCMs are called HadGEM, GFDL and MIROC and correspond respectively to an average, dry and wet scenario. These three GCMs were chosen because they are the ones for which the data was already available from Inge de Graaf's runs. In these projections data, a "business-as-usual" scenario is assumed meaning that the industrial and domestic water demands stay constant over time and that the irrigation demands is only a function of the climate (Graaf (de) et al.,submitted). The "business-as-usual" scenario means that in these runs, only the influence of climate is taking into account. The result of these three different scenarios will be analysed in order to know where and when the most of the changes are to be expected. These GCMs are runs for different atmospheric and oceanic circulation scenarios, therefore they give different results. Analysing the results of these three GCMs allows us to know what are the possibility range of area of gaining, losing and disconnected (intermittently and contnuously) streams in the future. An uncertainty analysis based on their variation overlap is made. The word uncertainty here relates to uncertainty of stream management.

This uncertainty is determined by comparing the moving average over 5 years of the area at the beginning (2010) for each type of streams with the moving average over 5 years of the area at the end and say what percentage decrease or increase was observed. On figure 20 the moving average over 5 years and the uncertainty bounds for each state of each GCMs are plotted. The upper uncertainty bounds were computed by calculating the standard error of each 5-years average and by adding the value to the 5-years average whereas the lower uncertainty bounds were computed by subtracting the standard error from the 5-years average.

As the historic runs and future runs were not run with the same forcing data, they are not comparable. Only the historic runs between each other and the future runs between each other can be compared. If we tried to compare them together the transition between the historic and future period is not smooth. In order to remedy that the reference run was made. In this run the model is run from 1950 to 2099 with the HadGEM GCM as forcing data. The mask chosen was different from the other run because it was not run first for the entire world (in order to decrease computation time), but only for North America and the mask needed to be hydrologically sound, meaning that it takes into account all a watershed and never just part of it. The mask is composed of the US and the North of Mexico. It is important to compare historic period with future period as it will show what extent and rate of changes can be expected compared to now. For the reference run an analysis on three 30-year periods (1955-1985, 2000-2030 and 2060-2090) in the changes of stream states is made. A 30-year period was chosen because it is usually on a 30-year period that climate studies are done. This analysis allows us to know where and when changes happened or are likely to happen in the future and to which degree. It allows us also to compare changes per season. The seasons were classified as December, January and February for winter, March, April and May for spring, June, July and August for summer and finally September, October, November for Autumn. To see the changes per season allow us to know which season are affected by those changes in stream states and therefore it can give an insight on the reason of these changes.

In figure 4 a summary of the method applied in order to get quantitative and spatial information about area of gaining, losing, intermittently disconnected and continuously disconnected streams is displayed as a flowchart for each run. First the groundwater head and the river head from the river bottom that we have computed before is available on a netCDF file. In order to make them easier to work with python, they are transformed into map files. This gives us a map file for every month for every years. The PCRaster (Karssenberg et al. , 2010) commands "clump" and "areaaverage" are used in a bash file in order to apply it to every map. These commands average the water head for each stream segment. Only the streams higher than order 2 were taken into account because streams of order 1 and 2 are too small to have an importance into the changes of stream states. The stream order are classified according to Strahler's method (1957). Then, using PCRaster, the groundwater head is compared to the river head and to the river bottom, in order for the stream to be classified as gaining, losing or disconnected. To distinguish between intermittently and continuously disconnected, a python script (final3map.py in the appendices section D) look at if it is 24 months in a row that the groundwater is disconnected from the stream. Then this data was exported to Excel, in order to make graphs.

For each run, graphs of the cumulative area of a stream order broken down into gaining, losing, intermittently

disconnected and continuously disconnected streams were created. To show the cumulative area per stream order, enables us to know if each stream order acts in the same way or not, and if they do not, which stream orders are the most at risk or least at risk, this can help to devise a suitable protection strategies. For each run, maps showing stream states for the same month of three different years are available as well as maps showing where streams are drier or wetter when comparing two different years. It is well acknowledged that comparing a single month with another single month is not really relevant, but an average over many years could not be done because of our definition of continuously disconnected streams. It was considered that as many years pass in between the compared month, most of the visible changes were still representative of the changes happening in between these years.

2.5 Validation of the model

It is important to first validate the model in order to know at which extend we can rely on its simulated data. In order to validate the model we decided to compare observed with simulated time series of groundwater level and surface water discharge for the Upper Arkansas catchment. For each comparison between observed discharge and simulated discharge, the correlation coefficient (r), the determination coefficient (R2), the Kling-Gupta Efficiency (KGE) and the percentage of bias (Pbias) is computed with the R logicial (Core_Team , 2008) function "gof" (for Goodness-Of-Fit). For each comparison between the observed and simulated groundwater level, the determination coefficient (r2) is computed in excel. Because of the manipulation done and explained later on the groundwater level time series, it does not make sens to compute the KGE or the Pbias.

The determination coefficient shows how much of the variance of the simulated time series is explained by the variance of the observed time series. It gives a measure on how well the observation are simulated by the model. It ranges between 0 and 1.

The correlation coefficient is a measure of the linear correlation between two variables in this case observed and simulated discharge. The correlation coefficient can have a value between 1 and -1, where one means that there is a positive linear correlation, -1 means that there is a negative linear correlation and 0 means that there is no linear correlation.

The Kling-Gupta efficiency (Gupta et al. , 2009) can be between -infinity and 1. Closer it is to one, better is the fit. It take into account the difference between the observed and simulated mean, the difference between the observed and simulated variance and the correlation coefficient.

The percentage of bias shows if the model is an overestimation (positive value) or an underestimation (negative value) of the observations. Closer it is to zero, better is the estimation.

2.5.1 Study Area

The study area is a part of the Upper Arkansas catchment (figure 5) and it is located in the USA in the states of Kansas and Oklahoma. The stations used for the validation are located on the rivers: Arkansas, Cimarron, Ninnescah, Chiskaskia, Walnut, Walnut C , Saltfork and Pawnee. This location was chosen because of the fact that there were enough gauging and well stations that were monitored for a long time but also because it is at the intersection between the dry part (West) and wet part (East) of North-America. As it is at the intersection area it is there that we can expect to observe the most of changes.

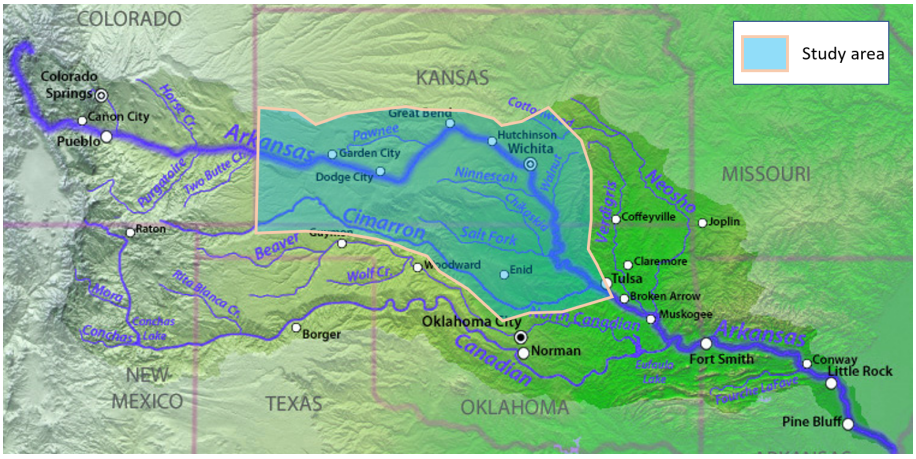

Figure 5: Upper Arkansas watershed with the study area highlighted in blue.

2.5.2 Surface water discharge

For assessing the performance of the simulated river discharges, 21 gauging stations spread across the study area were chosen from the USGS website. The stations with available and long enough monthly discharge statistics were chosen. The observed data was compared with the simulated data of the 5 arcminut cells that were the nearest and has the same drainage area as the station. The duration of the time series varies from 11 to 70 years. The time series of observed and simulated discharge are in the appendix on figures B.1, B.2 and B.3.

2.5.3 Groundwater level

For assessing the performance of the simulated groundwater level, 19 well stations spread across the study area were chosen from the USGS website. These stations were chosen upon the duration of the observation period. Most of the stations had maximum four observations a year whereas the simulation gives us 12 observations a year, one for each month. Moreover, the observed groundwater level is a punctual observation which the value depends on the elevation of the piezometer location whereas the simulated groundwater level is an average over a 5 arcmin cell. In order to make the simulated and observed time series more comparable with each other, we decided to compare the trends of the time series by removing the mean (which affects the KGE). The duration of the compared time series varies from 20 to 70 years depending on the observation period of the stations. The observed time series were compared with the simulated times series `groundwaterDepthLayer` computed previously by Edwin Sutanudjaja via PCR-GLOBWB. These times series are in the appendix on figures B.4, B.5. To compute the determination coefficient, the observed data was compared with the simulated for which the date was the nearest to the date of the measurement.

3 Results

3.1 Validation of the model

The determination coefficient for the comparison of the surface water (SW) discharge between the gauging station and the PCR-GLOBWB model ranges between 0.017 and 0.436 and are displayed on figure 6. The best of them are situated on Arkansas, Cimarron and Saltfork rivers and are written in green on the table of figure 6. The times series are displayed in the appendix on figures B.1, B.2 and B.3. The simulated discharges usually show more variation than the observed ones and appear to overestimate the discharge compare to the observations. Only the WALN (fig.B.2), NIN3 and NIN3 (fig.B.3) stations show more discharge for the observation than for the simulation.

The determination coefficient for the comparison of the monthly groundwater (GW) level between the wells station and the model range between 0.003 and 0.63 and are displayed on figure 7. The times series of the data used for computed the determination coefficient are displayed in the appendix on figures B.4 and B.5. The observed groundwater levels show more variations overall than the simulated ones except for CIM3 (fig.B.4), ARK4, CIM4 and CIM5 (fig.B.5) were the simulated groundwater level is varying a lot more than the observed one.

Even if the determination coefficient reach a higher score for the groundwater level, it is still the surface water discharge that show a better correlation between observed and simulated data. Indeed, for four well stations the correlation between observed and simulated are negative. These stations are NIN1, NIN2, CIM3 and CIM2. Also for the groundwater level, 10 stations out of 19 show a determination coefficient that is lower than 0.1 whereas for the surface water discharge 6 water stations out of 21 are have a determination coefficient lower than 0.1.

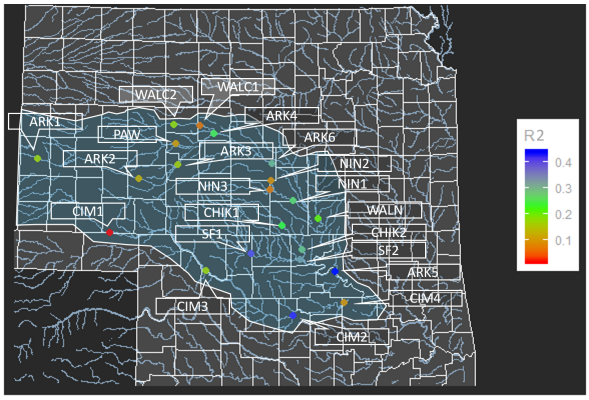

Name	ID	drainage area (km²)	IDENT	LAT	LONG	R2	R	KGE	PBIAS (%)
ARKANSAS R AT SYRACUSE, KS	07138000	6.19E+04	ARK1	37.97	-101.76	0.16	0.4	-2.87	3.73
ARKANSAS R AT DODGE CITY, KS	07139500	6.48E+04	ARK2	37.74	-100.03	0.1156	0.34	-9.46	9.93
ARKANSAS R NR KINSLEY, KS	07140000	7.10E+04	ARK3	37.93	-99.37	0.1521	0.39	-10.12	10.28
ARKANSAS R AT GREAT BEND, KS	07141300	7.34E+04	ARK4	38.35	-98.76	0.25	0.5	-6.54	7.03
Arkansas River at Ralston, OK	07152500	1.21E+05	ARK5	36.5	-96.73	0.4356	0.66	-0.09	1.02
ARKANSAS R NR HUTCHINSON, KS	07143330	8.22E+04	ARK6	37.95	-97.77	0.3025	0.55	-4.04	4.55
CHIKASKIA R NR CORBIN, KS	07151500	2.06E+03	CHIK1	37.13	-97.6	0.2401	0.49	-0.99	1.72
Chikaskia River near Blackwell, OK	07152000	4.85E+03	CHIK2	36.81	-97.28	0.2916	0.54	-0.48	1.35
Cimarron River near Forgan, OK	07156900	1.35E+04	CIM1	37.01	-100.49	0.0169	0.13	-11.87	9.18
Cimarron River near Guthrie, OK	07160000	3.35E+04	CIM2	35.92	-97.425	0.4225	0.65	-0.78	1.53
Cimarron River near Waynoka, OK	07158000	2.43E+04	CIM3	36.51	-98.88	0.16	0.4	-1.58	2.42
Cimarron River at Oilton, OK	07163500	3.56E+04	CIM4	36.09	-96.58	0.09	0.3	-1.26	1.97
PAWNEE R AT ROZEL, KS	07141200	5.21E+03	PAW	38.21	-99.41	0.0961	0.31	-3.88	4.73
Salt Fork Arkansas River nr Jet, OK	07150500	8.27E+03	SF1	36.75	-98.13	0.3969	0.63	-0.92	1.84
Salt Fork Arkansas River at Tonkawa, OK	07151000	1.16E+04	SF2	36.67	-97.31	0.3249	0.57	-0.42	1.33
WALNUT R AT WINFIELD, KS	07147800	4.87E+03	WALN	37.22	-96.99	0.2025	0.45	0.21	-0.24
WALNUT C AT ALBERT, KS	07141900	3.75E+03	WALC1	38.46	-99.01	0.0625	0.25	-2.93	3.72
WALNUT C AT NEKOMA, KS	07141780	2.98E+03	WALC2	38.47	-99.44	0.1681	0.41	-7.96	8.37
NINNESCAH R NR PECK, KS	07145500	4.62E+03	NIN1	37.46	-97.42	0.2704	0.52	0.16	0.64
NINNESCAH R AT CHENEY DAM, KS	07144795	1.72E+03	NIN2	37.72	-97.79	0.0841	0.29	0.13	0.4
NINNESCAH R NR MURDOCK, KS	07145200	1.46E+03	NIN3	37.6	-97.8	0.0676	0.26	0.05	-0.48

Figure 6: Determination coefficient between the trends of the simulated and observed discharge time series for 21 gauging stations located in Kansas and Oklahoma

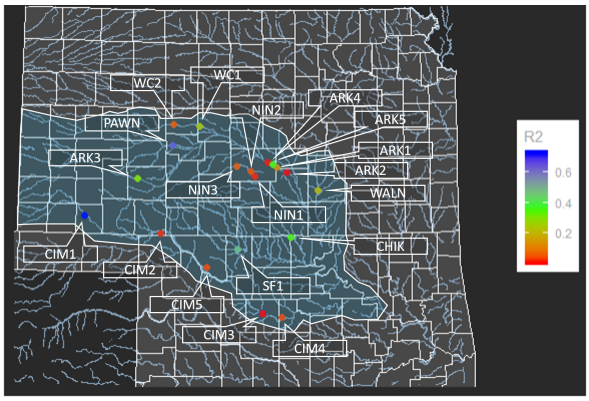

Name	ID	IDENT	LAT	LONG	Well depth (m)	r	R^2
24S 03W 31DDD 02 892	375448097405502	ARK1	37.9125	-97.6839	31.70	0.36	0.1272
26S 25W 34BBB 01	374445100025501	ARK3	37.7458	-100.0486	6.19	0.53	0.2849
26S 07W 14BBB 02	374726098034502	NIN1	37.7913	-98.0636	32.00	-0.12	0.0149
24S 10W 36AAA 02	375532098214702	NIN3	37.925	-98.363	NA	0.24	0.0564
32S 33W 21CDB 01	371444100550101	CIM1	37.2455	-100.917	16.15	0.85	0.7229
35S 21W 07AAA 01	370107099375501	CIM2	37.0186	-99.6319	10.09	-0.14	0.0204
17N-07W-11 DCD 2	355724097544001	CIM3	35.958	-97.9128	10.06	-0.05	0.0026
29N-02W-19 CDC 1	365824097272901	CHIK	36.9714	-97.4566	NA	0.58	0.3382
21S 19W 30BCC 01	381147099272701	PAWN	38.1964	-99.4575	22.13	0.79	0.6313
27N-11W-14 DBB 1	364909098210301	SF1	36.8191	-98.3508	11.28	0.69	0.4759
18S 15W 28CCC 03	382704098593803	WC1	38.4511	-98.9939	20.79	0.48	0.232
18S 19W 20ADD 01	382821099262301	WC2	38.4725	-99.4397	16.76	0.24	0.0574
28S 04E 21AAA 01	373624096591901	WALN	37.6067	-96.9886	17.43	0.44	0.1978
25S 02W 26CCBD02	375032097305902	ARK2	37.8422	-97.5164	59.44	0.09	0.0088
24S 05W 11AAAA02	375902097495202	ARK4	37.9839	-97.8311	76.20	0.11	0.0118
24S 04W 22ABBB02	375722097444902	ARK5	37.9561	-97.7469	65.84	0.58	0.339
17N-04W-34 ABB 1	355441097363901	CIM4	35.9114	-97.6108	NA	0.20	0.0389
24N-16W-01 DCC 1	363446098514101	CIM5	36.5794	-98.8614	24.38	0.19	0.0365
25S 07W 29BBB 01	375111098072001	NIN2	37.854	-98.1231	9.14	-0.21	0.0452

Figure 7: Determination coefficient between the trends of the simulated and observed groundwater level time series for 19 well stations located in Kansas and Oklahoma

3.2 Groundwater-streamflow interactions

To investigate the interaction between surface water and groundwater over time under the influence of climate variability and climate change, the classification of figure 1 with the disconnected class split into intermittently and continuously disconnected, was applied to river segments representing different Strahler stream orders (Strahler , 1957) for different scenarios. These scenarios were evaluated with the coupled version of PCR-GLOBWB and MODFLOW (Sutanudjaja et al. , 2018) for North America. These scenarios comprise a naturalised and two human influenced runs for the historic period and a future run using the forcing of 3 GCMs under RCP8.5 (HadGEM, GFDL and MIROC). The non-natural historic scenario from Edwin is the one that was run for North America and for the world. These different runs were started for different initial conditions and were not consistent over the transition from the historical runs, observed climate and the projected future ones. To overcome this, a consistent reference run using both the historic period and future climate forcing of HadGEM bias-corrected (Hempel et al. , 2013) was used as reference.

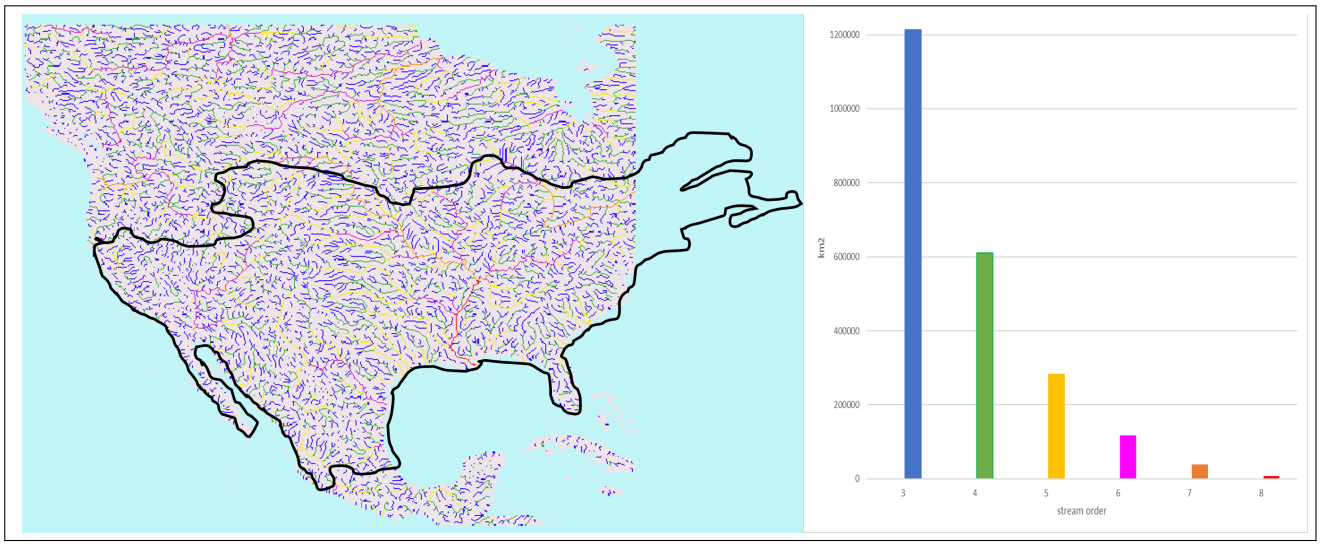

Figure 8: Map representing the mask used to describe the result of all scenarios (historic and future) and the mask for the reference run is represented with the black contour. It shows all the stream order higher than 2 (classified according to Strahler stream order) and their abundance.

3.2.1 Historic Period

In this section the quantitative and qualitative changes of the runs for the historic period will be analysed and compared for the period 1961-2004. The characteristics of theses runs are cited in table 1. It is interesting to compare the two Non-Natural runs together in order to see the changes triggered by the use of two different CRUs (Climatic Research Unit). And it is interesting to compare the Non-natural runs with the Natural run in order to know what changes are due only to climate and what changes are enhanced by human's influence.

On figure 9, the time series of the gaining, losing, intermittently disconnected and continuously disconnected streams area are displayed for the historic runs: Natural Inge, Non-natural Inge and Non-natural Edwin. This graph allows us to compare the global trends of each run. The reference run is not present in this graph because of its spatially different mask. On table 2, the slope of the trends of each type of stream for each run between the year 1961 and the year 2004 is revealed. These two figures enable a quantitative comparison of the global trend of each historic run for North-America.

The Natural run from Inge shows an increase in gaining streams and a decrease in all other types of streams. It is thus becoming wetter in this scenario. The Non-natural run from Inge shows an increase in gaining and continuously disconnected streams and a decrease in losing and intermittently disconnected streams. As the increase in gaining streams is 30 times faster than the increase in continuously disconnected streams (table 2), North-America is becoming wetter in this scenario too. The Natural-run from Edwin shows an increase in gaining and intermittently disconnected streams and a decrease in losing and continuously disconnected streams. As gaining streams increase and continuously disconnected streams decrease, it can be considered that North-America is also becoming wetter in this scenario. The historic period of the reference run shows another trend. Indeed in this scenario, intermittently and continuously disconnected streams increase whereas gaining

and losing streams decrease. As gaining stream area decreases at the same rate as continuously disconnected streams area increases, North-America is becoming drier in this scenario.

Figure 10 points out, for each run, where the changes occur. These maps only compare June 1964 with June 1984 and June 1984 with June 2004. For each run, maps showing the evolution of states of streams between these 3 months are displayed in the appendix (Figures C.1, C.2, C.3 and C.4). The areas of changes between each run can be compared on this figure. It is clear that the Natural, Non-natural run from Inge and Non-natural run from Edwin show that the changes occur in the same areas, whereas the reference run does not show similar results. The Missouri stream that is a stream of order 7 becomes drier for the first three runs (Natural Inge, Non-natural Inge, Non-natural Edwin) as well as streams in Montana, North Dakota, north of South-Dakota and west of Minnesota. Therefore, most of the drier streams are situated in the North of the great plain region in the US. All of these three runs also show that the border between Mexico and Guatemala becomes drier. There are some divergences between these three runs too. Only Edwin's run shows that the end of the Mississippi river becomes drier. The non-natural and natural run of Inge show more drier streams in south of Canada. The common areas that become wetter are the south-west of Canada, north of Nevada, Idaho, north of California, Oregon and Utah, these areas are located in the north of the Intermountain Plateau and Pacific Mountains areas. The tributaries of the Missouri river in Missouri and Arkansas also become wetter in these three runs. The reference run, for the area that can be compared, shows a totally different result. Indeed the only wetter streams are mainly between the middle of Nebraska and the middle of South-Dakota. The drier streams are mainly located on the Great Plains area and around the border between Great Plains and Intermountain plateau.

It is also visible on figure 10 that for the first three runs, it is globally long segments of streams that become drier and shorter ones that become wetter. It does look like streams of smaller order are becoming wetter and streams of higher order are becoming drier. For the reference run, almost all changes shown are toward a drier state of stream no matter the order. In order to analyse that, figure 11 and table 3 were made. Figure 11 only shows for streams of order 3, 5 and 7. This is done because it is considered that streams of order 4 acts like streams of order 3, streams of order 6 like streams of order 5 and streams of order 7 like streams of order 8. The same figure but for stream of order 4, 6 and 8 is displayed in the appendix (Fig.C.5). Indeed we can see on figure 11, that for the first three runs (Natural and Non-natural from Inge and Edwin), the area of gaining streams increases whereas the area of continuously disconnected streams, and losing streams decreases for streams of order 3. For streams of order 5, the area of gaining streams decreases and the area of losing stream increases for Inge's runs but not for the Non-natural run from Edwin where the area of gaining streams increases and the area of losing streams decreases. However, the area of continuously disconnected streams does increase for the streams of order 5. For the streams of order 7, the area of gaining streams decreases for the two Inge's runs and increases for Edwin's run. The reference run shows an other behaviour for all states of streams compared to the first three runs. Indeed for streams of order 3 and 5 it shows a decrease in gaining streams and an increase in losing and continuously disconnected streams. Most of the streams of order 7 are gaining, except for a small area that is losing at the beginning and after changes into intermittently, then continuously disconnected streams.

These figures enable us to compare the Natural run with the Non-natural runs in order to have an insight on where climate and humans have the biggest influence. On figure 10, there are almost no detectable differences between the Natural run and Non-natural run from Inge. We can only see that there are more wetter streams in the north of Texas and less drier streams in south of Nebraska for the Natural run. Table 2 shows that there is a difference, indeed for the Natural run, there is a decrease in continuously disconnected streams whereas there is an increase for the Non-natural run from Inge. Figure 10 shows that the Natural and Non-natural run from Inge show a similar pattern for each stream order but there are more gaining streams in the Natural run than in the Non-natural run. When comparing the Natural run from Inge and the Non-natural from Edwin, it is clear that there is less streams that become drier between June 1964 and June 1984 and more streams that become drier between June 1984 and June 2004 from Edwin's run. Between June 1984 and June 2004 it is drier around the border between Nebraska and South Dakota for both Non-natural runs but not for the Natural run. Table 11 shows that the increase in gaining stream for Edwin's run is three time steeper than for the natural run whereas the decrease in continuously disconnected streams is 10^5 m^2/month smoother. Also there is an increase in intermittently disconnected streams for the Non-natural run of Edwin whereas it is a decrease for the Natural run. The run from Edwin shows a similar behaviour as the Natural run for streams of order 3 but not for streams of order 5 neither 7. Figure 9 shows that there are more gaining streams and less intermittently and continuously disconnected streams in the Natural run than in both Non-natural runs.

When comparing the two Non-natural runs together, it is clear that their extent of changes and their trends are not the same whereas the areas that are becoming drier and wetter are similar, only the extent is different. The amount of gaining and losing streams shows a similar trend, although not a similar rate. The amount of

intermittently and continuously disconnected streams reveals opposite trends (Fig.2). There are less gaining, intermittently and continuously disconnected streams and more losing streams for Inge's run. Also streams of order 5 and 7 behave oppositely for these two runs.

Table 3 shows the percentage of increase between June 1964 and June 1984 and for June 1984 and June 2004 for streams of order 3, 5 and 7. We can see that these percentages of change do not always match with the trends seen in table 11. This table allows us to see if the changes displayed in figure 10 are due to an increase/decrease of gaining, losing, intermittently disconnected, continuously disconnected streams.

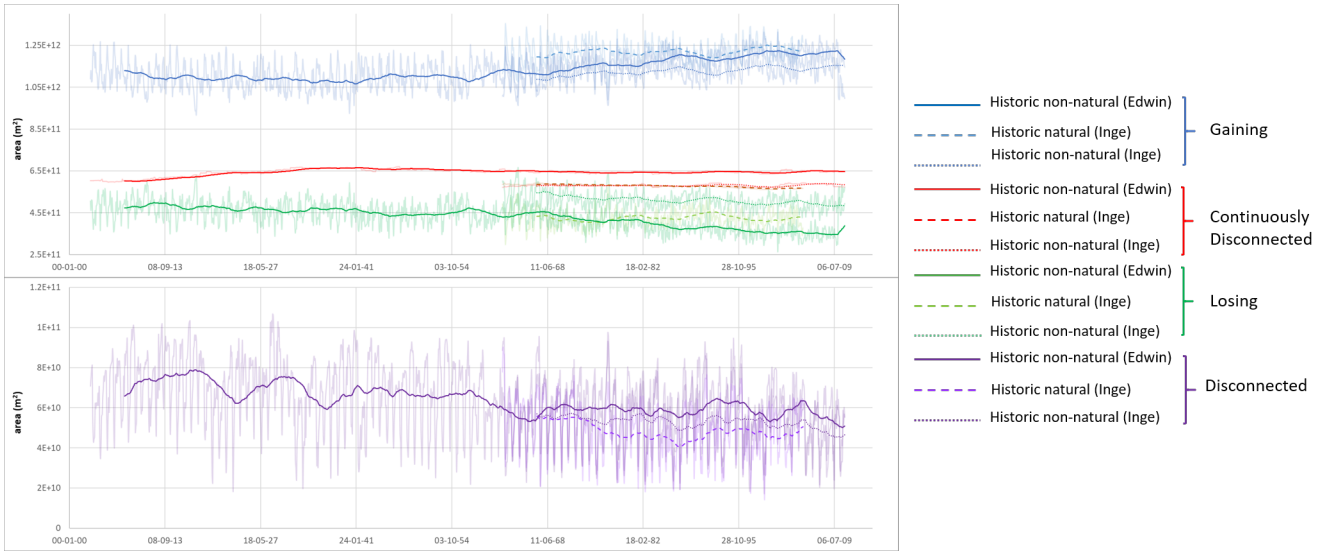

Figure 9: Moving average over 5 years of area of gaining, losing, intermittently disconnected and continuously disconnected streams over time for the runs : Natural Inge, Non-natural Inge and Non-natural Edwin.

Table 2: Slope of each type of stream trend, show in figure 9 (except for the reference run) between 1961 and 2004, green shows a negative trend and red a positive trend.

Run Name	Slope trend of gaining streams (m²/month)	Slope trend of losing streams (m²/month)	Slope trend of intermittently disconnected S. (m²/month)	Slope trend of continuously disconnected S. (m²/month)
Natural Inge	2E+6	-3E+4	-5E+5	-1E+10
Non-natural Inge	3E+6	-3E+6	-3E+5	1E+5
Non-natural Edwin	7E+6	-7E+6	2E+5	-1E+5
Reference	-3E+6	-4E+5	3E+5	3E+6

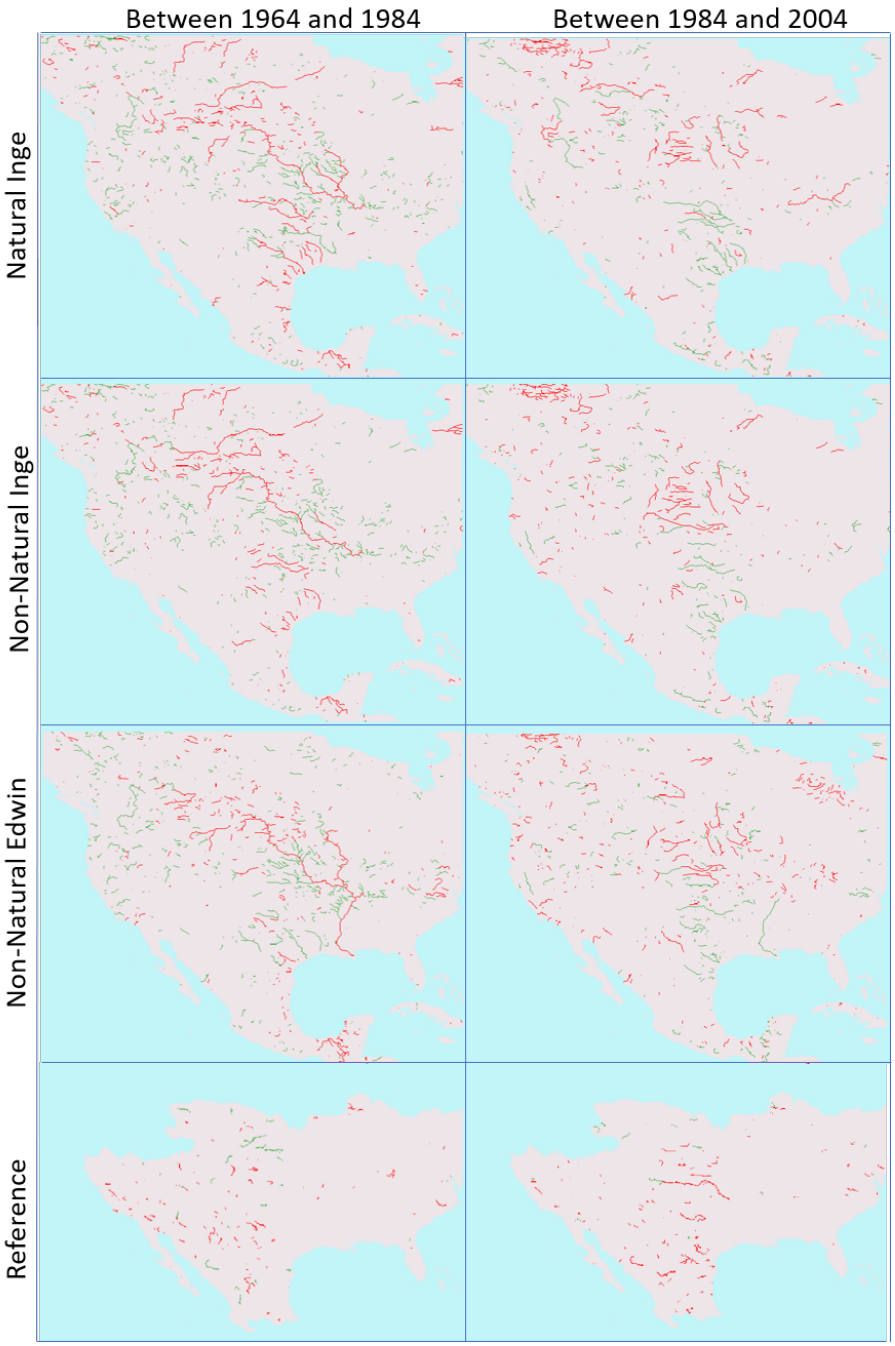

Figure 10: These maps show where the changes to a drier (red) or wetter (green) state of streams happens for each historic run. The first row shows the changes between June-1964 and June-1984 and the second row shows the changes between June-1984 and June-2004.

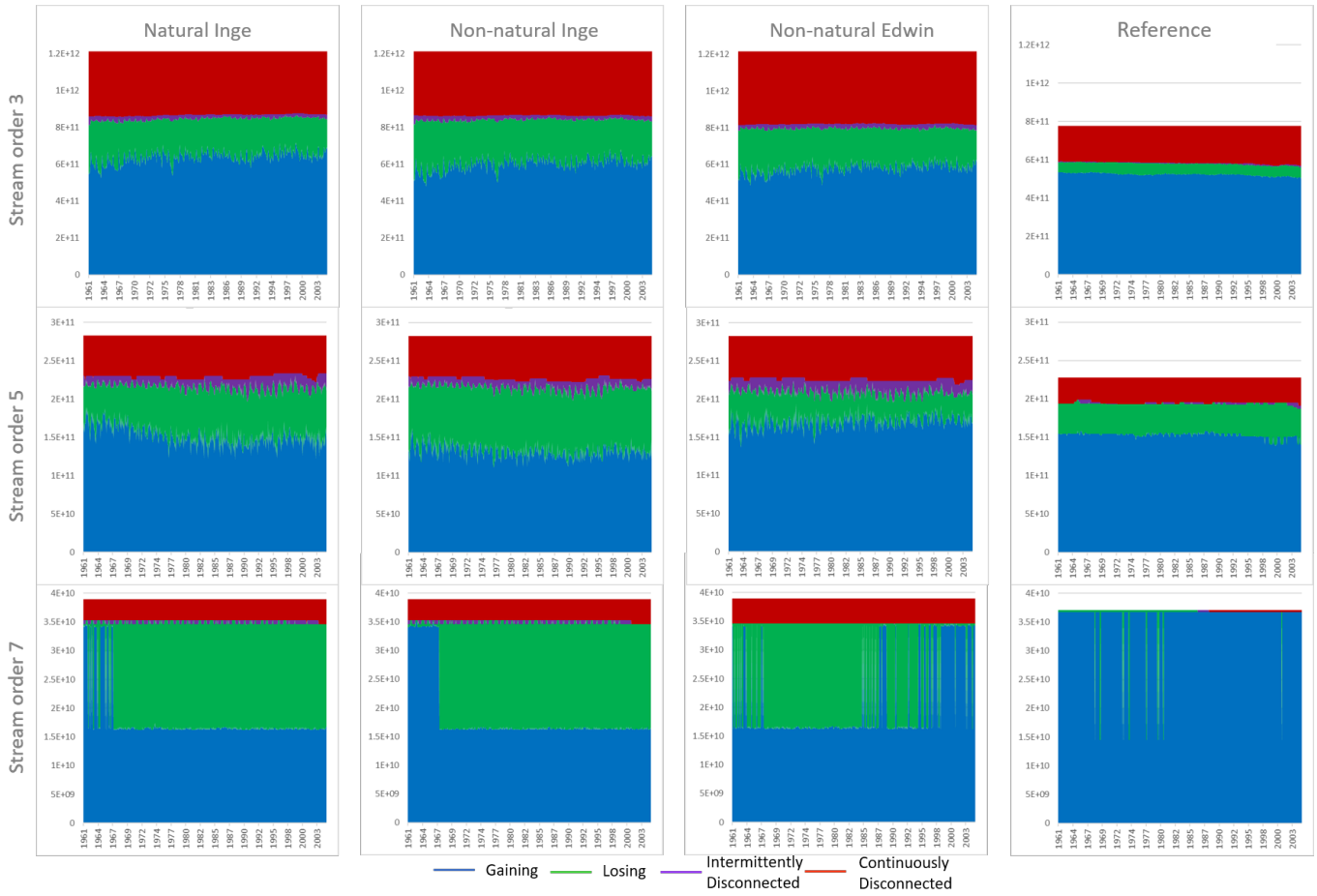

Figure 11: Comparison in area (m^2) between the change of state of stream for the different historic runs. The graph represent the cumulative area of stream of order 3, 5 and 7. The graphs for the streams of order 4,6 and 8 are in the appendix (Fig.C.5)

Table 3: Percentage of changes in areas of gaining, losing, intermittently and continuously disconnected streams for the dates June-1964, June-1984 and June-2004 for every historic run. Increase of area in red, decrease of area in green.

Name	Type of stream	Date	Stream of order 3 (m2)	% of changes (SO3)	Stream of order 5 (m2)	% of changes (SO5)	Stream of order 7 (m2)	% of changes (SO7)
Natural Inge	Gaining	1964-06	6.34E+11		1.69E+11		3.43E+10	
		1984-06	6.93E+11	9.31	1.42E+11	-15.98	1.65E+10	-51.90
		2004-06	6.93E+11	0.00	1.43E+11	0.70	1.62E+10	-1.82
	Losing	1964-06	2.11E+11		5.61E+10		1.06E+09	
		1984-06	1.66E+11	-21.33	8.04E+10	43.32	1.88E+10	1673.58
		2004-06	1.61E+11	-3.01	7.13E+10	-11.32	1.84E+10	-2.13
	Intermittenly disconnected	1964-06	1.69E+10		4.39E+09		0.00E+00	
		1984-06	1.20E+10	-28.99	7.12E+09	62.19	0.00E+00	0.00
		2004-06	1.65E+10	37.50	1.94E+10	172.47	0.00E+00	0.00
	Continuously Disconnected	1964-06	3.51E+11		5.28E+10		3.65E+09	
		1984-06	3.42E+11	-2.56	5.28E+10	0.00	3.65E+09	0.00
		2004-06	3.43E+11	0.29	4.90E+10	-7.20	4.35E+09	19.18
Non-Natural Inge	Gaining	1964-06	2.56E+11		6.78E+10		1.06E+09	
		1984-06	1.95E+11	-23.83	8.03E+10	18.44	1.91E+10	1701.89
		2004-06	1.87E+11	-4.10	8.44E+10	5.11	1.84E+10	-3.66
	Losing	1964-06	5.93E+11		1.55E+11		3.43E+10	
		1984-06	6.57E+11	10.79	1.36E+11	-12.26	1.62E+10	-52.77
		2004-06	6.54E+11	-0.46	1.30E+11	-4.41	1.62E+10	0.00
	Intermittenly disconnected	1964-06	1.56E+10		7.10E+09		0.00E+00	
		1984-06	1.64E+10	5.13	1.08E+10	52.11	0.00E+00	0.00
		2004-06	2.10E+10	28.05	1.23E+10	13.89	0.00E+00	0.00
	Continuously Disconnected	1964-06	3.49E+11		5.28E+10		3.65E+09	
		1984-06	3.45E+11	-1.15	5.56E+10	5.30	3.65E+09	0.00
		2004-06	3.51E+11	1.74	5.61E+10	0.90	4.35E+09	19.18
Non-Natural Edwin	Gaining	1964-06	5.76E+11		1.71E+11		3.40E+10	
		1984-06	6.29E+11	9.20	1.78E+11	4.09	1.65E+10	-51.47
		2004-06	6.13E+11	-2.54	1.64E+11	-7.87	1.62E+10	-1.82
	Losing	1964-06	2.29E+11		4.61E+10		5.77E+08	
		1984-06	1.75E+11	-23.58	3.53E+10	-23.43	1.81E+10	3036.92
		2004-06	1.81E+11	3.43	4.28E+10	21.25	1.84E+10	1.66
	Intermittenly disconnected	1964-06	1.21E+10		1.16E+10		0.00E+00	
		1984-06	2.06E+10	70.25	1.45E+10	25.00	0.00E+00	0.00
		2004-06	2.09E+10	1.46	1.77E+10	22.07	0.00E+00	0.00
	Continuously Disconnected	1964-06	3.96E+11		5.45E+10		4.35E+09	
		1984-06	3.88E+11	-2.02	5.45E+10	0.00	4.35E+09	0.00
		2004-06	3.98E+11	2.58	5.79E+10	6.24	4.35E+09	0.00
Reference	Gaining	1964-06	5.30E+11		1.55E+11		3.67E+10	
		1984-06	5.26E+11	-0.75	1.56E+11	0.65	3.67E+10	0.00
		2004-06	5.06E+11	-3.80	1.41E+11	-9.62	3.67E+10	0.00
	Losing	1964-06	5.70E+10		3.90E+10		3.61E+08	
		1984-06	5.21E+10	-8.60	3.75E+10	-3.85	3.61E+08	0.00
		2004-06	6.01E+10	15.36	4.62E+10	23.20	0.00E+00	-100.00
	Intermittenly disconnected	1964-06	2.63E+09		0.00E+00		0.00E+00	
		1984-06	3.10E+09	17.87	2.27E+09	∞	0.00E+00	0.00
		2004-06	4.85E+09	56.45	4.48E+09	97.36	0.00E+00	0.00
	Continuously Disconnected	1964-06	1.87E+11		3.46E+10		0.00E+00	
		1984-06	1.95E+11	4.28	3.25E+10	-6.07	0.00E+00	0.00
		2004-06	2.06E+11	5.64	3.68E+10	13.23	3.61E+08	∞

3.2.2 Projections

In this section the quantitative and qualitative changes of the run for the future will be analysed and compared. As an increase in water demand is not accounted for, these runs are only looking at changes due to climate. It should not be forgotten that these scenarios were run under the 8.5 RCP. The characteristics of theses runs are cited in table 1.

On figure 12, the time series of the gaining, losing, intermittently and continuously disconnected streams area are displayed for the future runs: HadGEM, GFDL and MIROC. This graph enables us to compare the global trends of each run. The reference run is not present on this graph because of its spatially different mask. The slope of each run on the graph and the reference run, for the period from 2010 to 2099, is reported on table 4. These two figures allow a quantitative comparison of the global trend of each future run.

The HadGEM run shows a decrease in gaining streams and an increase in all other types of streams. North-America is becoming drier in this scenario. The GFDL run shows an opposite pattern as there is an increase in gaining streams and a decrease in all other types of streams. North-America is thus becoming wetter in this scenario. The MIROC run shows an increase in gaining streams and a decrease in continuously disconnected streams, therefore, North-America is becoming wetter in this scenario too. The reference run, that was also run with the HadGEM GCM, predicts that North-America is becoming drier as gaining streams decrease and continuously disconnected streams increase. It is interesting to notice that the increase in losing and intermittently disconnected streams is at the same rate as for the GFDL run.

Figure 13 displays for each run where the changes occur. These maps only compare June 2020 with June 2060 and June 2060 with June 2099. For each run, maps showing the evolution of states of streams between these 3 months are displayed in the appendix (Figure C.6, C.7, C.8 and C.9). One can see that the changes occur in the same areas for the first three projections but the changes are not towards the same trends. One can see that for GFDL and MIROC the changes are more or less the same between June 2020 and June 2060. Indeed for both runs, the south-west of Canada and west and north-west of the US become wetter overall with still some streams that become drier, more for MIROC than for GFDL. Whereas between June 2060 and June 2099, the changes for the MIROC run are more similar to the HadGEM run. Indeed, the south of Canada and the north-west of the US become drier as well as the south of Mexico. There are more streams that become drier for the HadGEM run than for the MIROC run. Also, one can notice that for the HadGEM run there are fewer changes between 2020 and 2060 than between 2060 and 2099 whereas the opposite is true for the GFDL run. For every run, there is at least a little part of Texas that becomes drier. The reference run, for area that we can compare, seems to show changes where the other runs do not. Between June 2020 and June 2060, its changes are closer from the GFDL run with less wetter streams. It shows drier streams in the south of the US Great Plains an in New-Mexico and Mexico and it shows wetter streams in the north of the US Great Plains.

An analysis on the influence of stream orders in the evolution toward a drier or wetter North-America was made for each run. Figure 14 and table 5 were made in order to compare the streams of order 3, 5 and 7 with each other and between runs. Figure C.10, in the appendix, is the same as figure 14 but for streams of order 4, 6 and 8. For stream order of 3 and 5 there are clear trends for every run except for MIROC. Indeed for HadGEM there is a decrease in gaining streams and an increase in losing and continuously disconnected streams for streams of order 3 and 5 whereas there are an increase in continuously disconnected streams and a decrease in gaining streams for GFDL run. The reference run shows a slight decrease in gaining streams, a decrease in losing streams and an increase in continuously disconnected streams which makes it more similar to the HadGEM run, which was expected. Every stream order for the same run shows the same trend, if there is one. For streams of order 7, the amount of losing streams decreases for GFDL and MIROC whereas the amount of gaining streams increases. For HadGEM the amount of losing streams of order 7 increases whereas the gaining streams decreases. It is interesting to notice that for the reference run, almost all streams of order 7 are gaining. Looking at figure C.10, one can see that for all scenarios, all streams of order 8 are losing.

Table 5 shows the percentage of increase between June 2020 and June 2060 and for June 2060 and June 2099 for streams of order 3, 5 and 7. We can see that these percentages of change do not always match with the trends seen in table 4. This table allows us to see if the changes displayed in figure 13 are due to an increase/decrease of gaining, losing, intermittently disconnected, continuously disconnected streams.

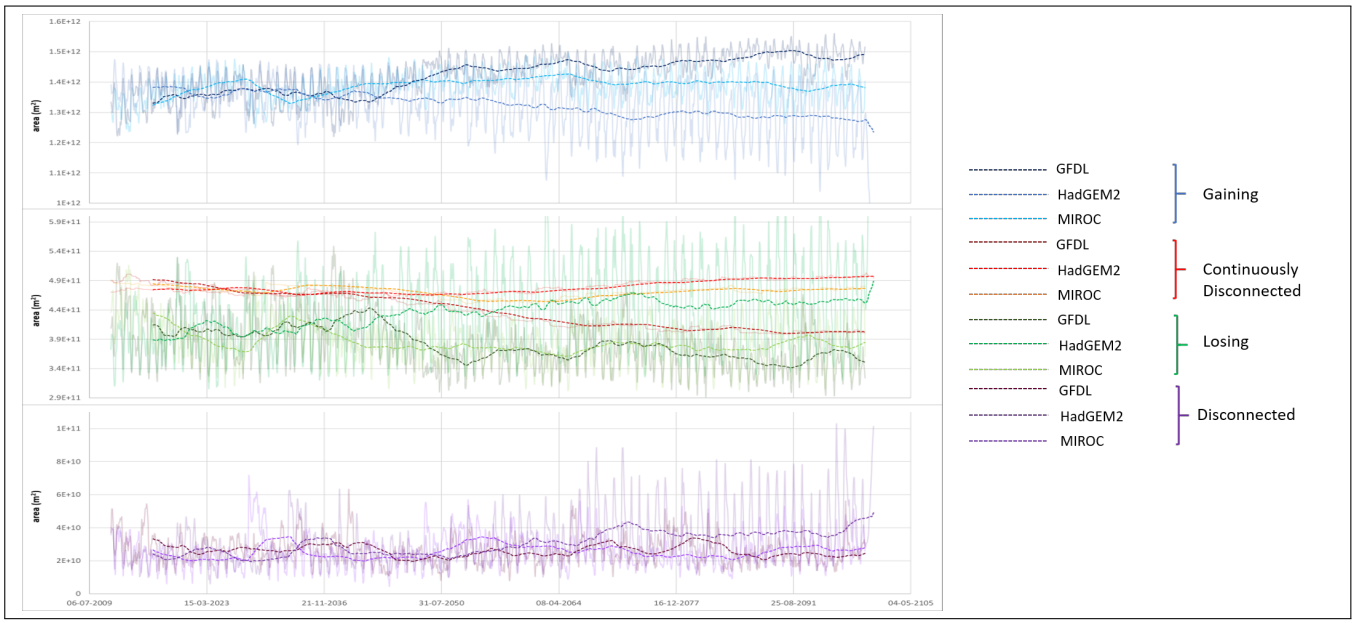

Figure 12: Moving average over 5 years (dashed lines) of area of gaining (blue), losing (green), intermittently disconnected (purple) and continuously disconnected (red) streams over time for the 3 GCMs: HadGEM (middle colour), GFDL (dark colour) and MIROC (light colour) for North America (fig.8). (Scale is not the same for each state of stream)

Table 4: Slope of each type of stream trend, show in figure 12 (except for the reference run) between 2010 and 2100, green shows a negative trend and red a positive trend.

Run Name	Slope trend of gaining streams (m^2/month)	Slope trend of losing streams (m^2/month)	Slope trend of intermittently disconnected S. (m^2/month)	Slope trend of continuously disconnected S. (m^2/month)
HadGEM	-4E+6	3E+6	7E+5	9E+5
GFDL	6E+6	-2E+6	-1E+5	-2E+6
MIROC	1E+6	-9E+5	7E+4	-2E+5
Reference	-5E+5	-2E+6	-1E+5	2E+6

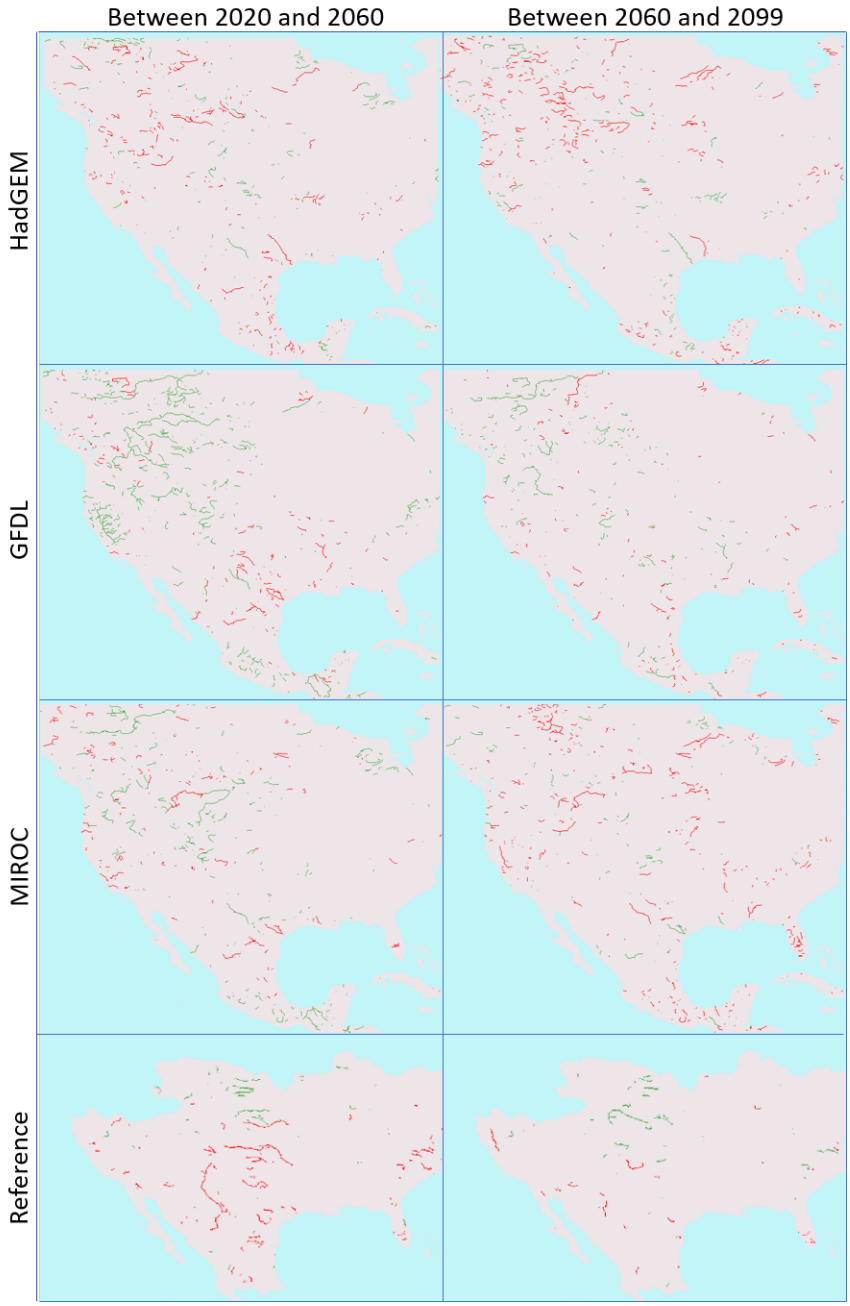

Figure 13: These maps show where the changes to a drier (red) or wetter (green) state of streams happens for each projection run. The first row shows the changes between June-2020 and June-2060 and the second row shows the changes between June-2060 and June-2099.

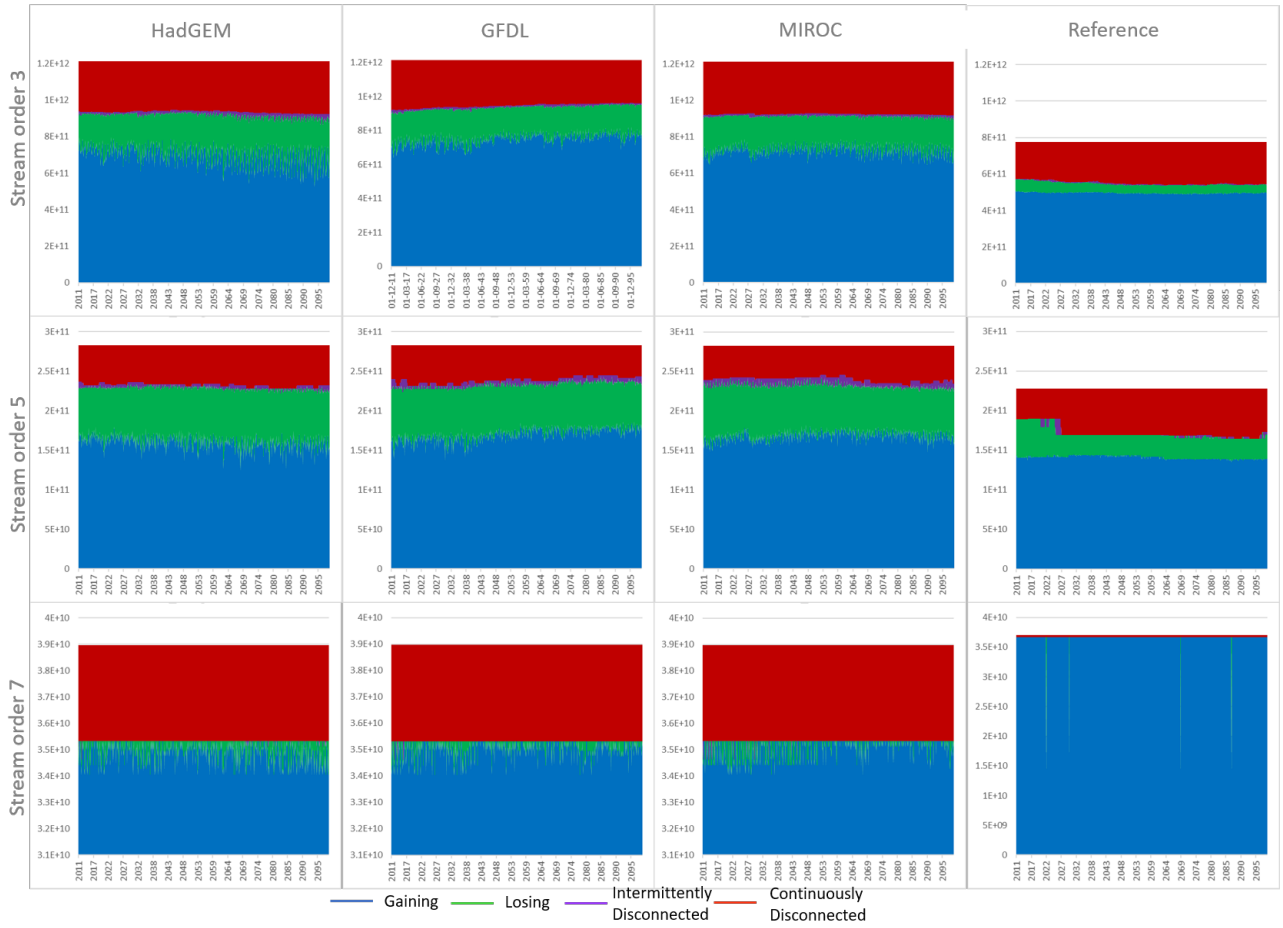

Figure 14: Comparison in area (m^2) between the change of state of stream for the different future runs. The graph represent the cumulative area of stream of order 3, 5 and 7. The graphs for the streams of order 4,6 and 8 are in the appendix (Fig.C.10)

Table 5: Percentage of changes in areas of gaining, losing, intermittently and continuously disconnected streams for the dates June-2020, June-2060 and June-2099 for every future run. Increase of area in red, decrease of area in green.

Name	Type of stream	Date	Stream of order 3 (m2)	% of changes (SO3)	Stream of order 5 (m2)	% of changes (SO5)	Stream of order 7 (m2)	% of changes (SO7)
HadGEM	Gaining	2020-06	7.53E+11		1.70E+11		3.50E+10	
		2060-06	7.30E+11	-2.98	1.59E+11	-6.57	3.50E+10	0.00
		2099-06	7.00E+11	-4.14	1.67E+11	5.06	3.51E+10	0.42
	Losing	2020-06	1.72E+11		6.03E+10		3.61E+08	
		2060-06	2.01E+11	16.91	7.13E+10	18.19	3.61E+08	0.00
		2099-06	2.08E+11	3.72	5.84E+10	-18.06	2.16E+08	-40.24
	Intermittenly disconnected	2020-06	1.06E+10		5.50E+09		0.00E+00	
		2060-06	1.36E+10	28.54	3.95E+09	-28.04	0.00E+00	0.00
		2099-06	1.53E+10	11.90	6.42E+09	62.39	0.00E+00	0.00
	Continuously Disconnected	2020-06	2.78E+11		4.66E+10		3.65E+09	
		2060-06	2.68E+11	-3.48	4.84E+10	3.78	3.65E+09	0.00
		2099-06	2.89E+11	7.87	5.08E+10	4.87	3.65E+09	0.00
GFDL	Gaining	2020-06	7.30E+11		1.61E+11		3.51E+10	
		2060-06	7.70E+11	5.42	1.76E+11	9.43	3.53E+10	0.62
		2099-06	7.78E+11	1.14	1.83E+11	3.90	3.53E+10	0.00
	Losing	2020-06	1.87E+11		7.07E+10		2.16E+08	
		2060-06	1.74E+11	-6.77	5.70E+10	-19.33	0.00E+00	-100.00
		2099-06	1.74E+11	0.05	5.21E+10	-8.67	0.00E+00	0.00
	Intermittenly disconnected	2020-06	8.87E+09		1.39E+08		0.00E+00	
		2060-06	6.30E+09	-28.95	7.85E+09	5551.77	0.00E+00	0.00
		2099-06	7.42E+09	17.62	8.43E+09	7.43	0.00E+00	0.00
	Continuously Disconnected	2020-06	2.87E+11		5.10E+10		3.65E+09	
		2060-06	2.63E+11	-8.48	4.17E+10	-18.11	3.65E+09	0.00
		2099-06	2.53E+11	-3.80	3.92E+10	-6.03	3.65E+09	0.00
MIROC	Gaining	2020-06	7.50E+11		1.71E+11		3.53E+10	
		2060-06	7.72E+11	2.95	1.78E+11	4.08	3.53E+10	0.00
		2099-06	7.28E+11	-5.67	1.68E+11	-5.51	3.53E+10	0.00
	Losing	2020-06	1.70E+11		6.81E+10		0.00E+00	
		2060-06	1.47E+11	-13.94	5.29E+10	-22.34	0.00E+00	0.00
		2099-06	1.80E+11	22.60	6.19E+10	17.16	0.00E+00	0.00
	Intermittenly disconnected	2020-06	4.98E+09		1.54E+09		0.00E+00	
		2060-06	6.77E+09	35.88	1.49E+10	869.92	0.00E+00	0.00
		2099-06	1.07E+10	58.61	4.34E+09	-70.93	0.00E+00	0.00
	Continuously Disconnected	2020-06	2.88E+11		4.19E+10		3.65E+09	
		2060-06	2.88E+11	-0.06	3.68E+10	-12.32	3.65E+09	0.00
		2099-06	2.94E+11	2.30	4.81E+10	30.85	3.65E+09	0.00
Reference	Gaining	2020-06	5.00E+11		1.41E+11		3.67E+10	
		2060-06	4.94E+11	-1.17	1.42E+11	0.38	3.67E+10	0.00
		2099-06	4.99E+11	0.96	1.39E+11	-2.26	3.67E+10	0.00
	Losing	2020-06	6.14E+10		3.80E+10		0.00E+00	
		2060-06	4.93E+10	-19.74	2.73E+10	-28.11	0.00E+00	0.00
		2099-06	4.52E+10	-8.41	3.13E+10	14.65	0.00E+00	0.00
	Intermittenly disconnected	2020-06	4.67E+09		1.05E+10		0.00E+00	
		2060-06	1.65E+09	-64.65	0.00E+00	-100.00	0.00E+00	0.00
		2099-06	1.68E+09	1.75	3.20E+09	∞	0.00E+00	0.00
	Continuously Disconnected	2020-06	2.11E+11		3.84E+10		3.61E+08	
		2060-06	2.32E+11	9.95	5.90E+10	53.71	3.61E+08	0.00
		2099-06	2.31E+11	-0.26	5.50E+10	-6.78	3.61E+08	0.00

3.3 30-year periods analysis of the reference run

This run is called the reference run because it was run continuously over time so that the transition between historical and future period is smooth which makes it the run to compare to the other runs. As shown in figure 8, the mask used is not the same as for the other historical and future runs. It is still North America but only the US (without Washington,Oregon and Idaho), a part of Quebec and the North part of Mexico.

This section has the purpose to show us the extent of the changes and where the changes happened and are predicted to happen for the reference run that was forced with the HadGEM GCM and calibrated with historical data. Three periods of 30-years are compared with each other, as it is more relevant to compare than three month with a time interval of 30 years. These periods are 1955 to 1985, 2000 to 2030 and 2060 to 2090. For this analysis, the disconnected streams are not split into intermittently and continuously.

Figure 15 shows the time series of changes in gaining, losing, intermittently disconnected and continuously disconnected streams from 1952 to 2099. The rate in the decrease of gaining streams area is at the same order of magnitude as the rate in increase of continuously disconnected streams. The decrease in gaining streams is sharp from 1952 to 2009 and after it decreases slightly until 2099 whereas the increase in continuously disconnected streams is continuous until 2050 when it starts to almost level off.

Figures 16 and 17 show where the changes happen and figures 18 and 19 show the changes in a quantitative way. Figure 19 also helps us to see how the seasons affect the changes of stream states. On figures 16 and 17, one can see that North-America (fig.8) becomes drier overall. Indeed the drier streams states spread from the west to the east but not further to the east than the line Kansas, Oklahoma, Texas. It is also spreading from North (starting at Nebraska, south of Wyoming latitude) to South (centre of Mexico). The east coast is becoming drier too, it is clearly visible for Florida. The streams going to a wetter state of streams are clustered well in the North of the map, namely in the area from North of Nebraska to South of South Dakota. The only stream of order 8 of the area studied (the Mississippi River) tends to change from gaining to losing or inversely depending on the season. Although in figure C.10, it is shown that there are only losing streams for streams of order 8 for the reference run. This is due to a difference of setting for when the river head is equal to the groundwater head. In the other analyses it was considered as still being losing whereas here it is considered to be gaining. It allows us to see that there is a difference between the season. This stream is apparently always "gaining" in winter and autumn and always losing in spring. Its behaviour for summer depends on the period.

On figure 18 it is clear that the area of gaining streams decreases over time, mainly comparing the periods 1955-1985 and 2000-2030. As the decrease in area of gaining streams is smaller between the period 2000-2030 and the period 2060-2090, we have to look at figure 19 to notice it. It is visible on figure 19 that spring is always the season with the smallest amount of gaining streams and in second position it is the summer season except for the last period when it is actually the season with the most area of gaining streams.

On figure 18 we can see that the area of disconnected streams increases steadily over time. Neither in figure 18 nor in figure 19 a change between seasons for the area of disconnected streams is noticeable.

We can notice on figure 18 that the area of losing streams varies but decreases overall. The variations are more striking on figure 19, where we can see that from the period 1955-1985 to the period 2000-2030 the area of losing streams increases, it is only for the last period (2060-2090) that a large decrease happens. Oppositely to the area of gaining streams, it is in spring that the area of losing stream is the largest and in second position it is summer except for the last period where winter is at the second position.

Figures 15 and figure 19 are highly similar if we compare the disconnected streams with the continuously disconnected streams. Indeed the trends for losing, gaining and disconnected streams are the same in these two figures.

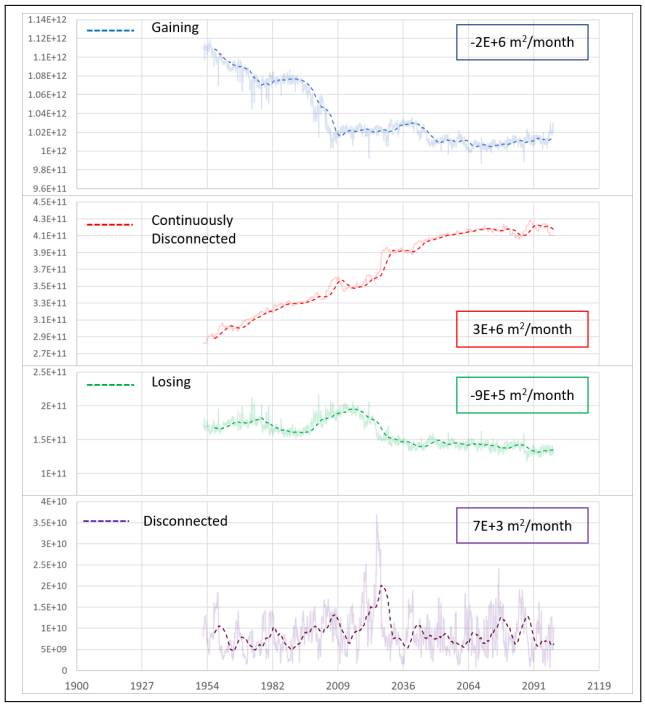

Figure 15: Moving average over 5 years (dashed lines), and the slope of the linear trend, of area of gaining (blue), losing (green), intermittently disconnected (purple) and continuously disconnected (red) streams over time for the reference for North America (fig.8). (Scale is not the same for each state of stream)

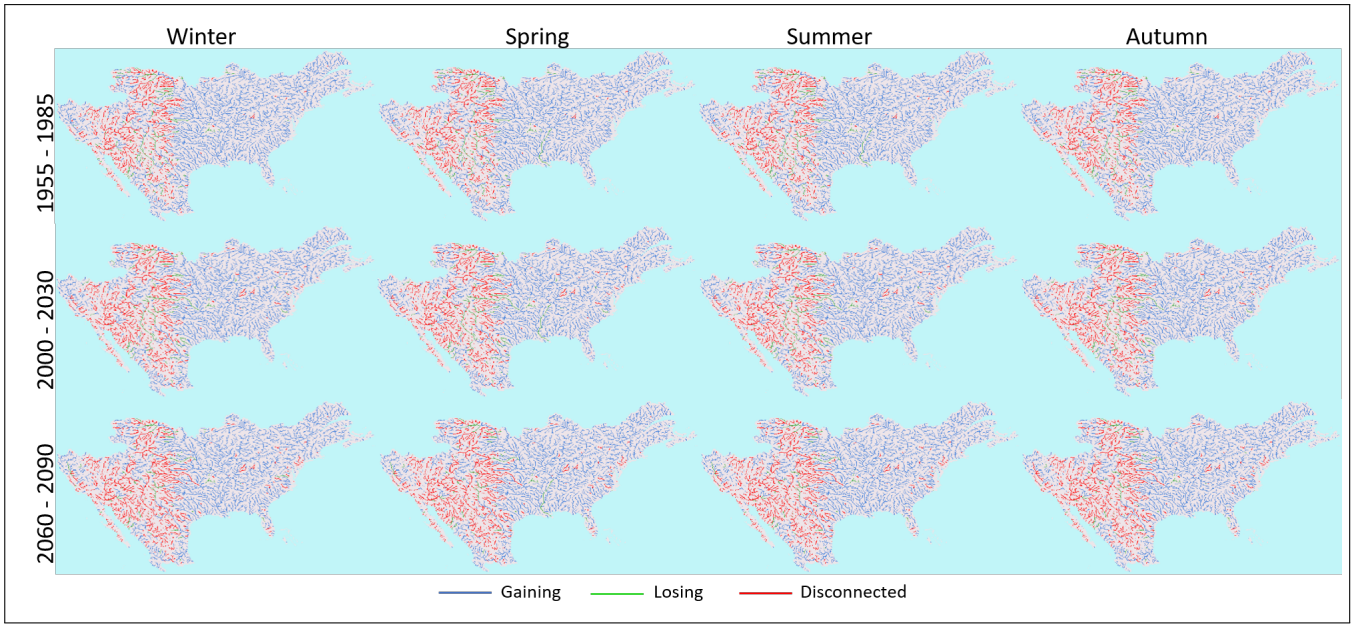

Figure 16: Maps of a part of North-America showing the location and propagation/reduction of gaining, losing and disconnected streams for winter, spring, summer and autumn averaged on a period of 30-year. 1^{st} row: 1955-1985, 2^{d} row: 2000-2030 and 3^{d} row: 2060-2090. This image is bigger in the appendix figure C.11

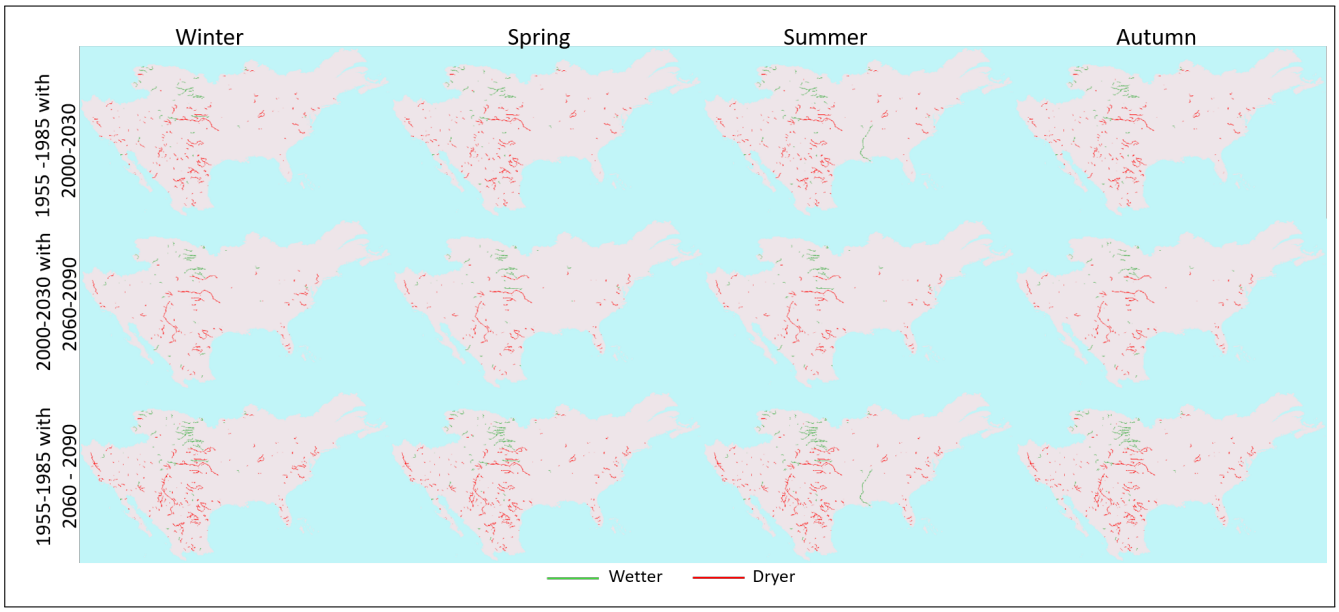

Figure 17: Maps of a part of North-America showing the location of drier (red) and wetter (green) streams comparing the 30-years period : 1^{st} row: 1955-1985 with 2000-2030, 2^{nd} row: 2000-2030 with 2060-2090 and 3^{rd} row: 1955-1985 with 2030-2060

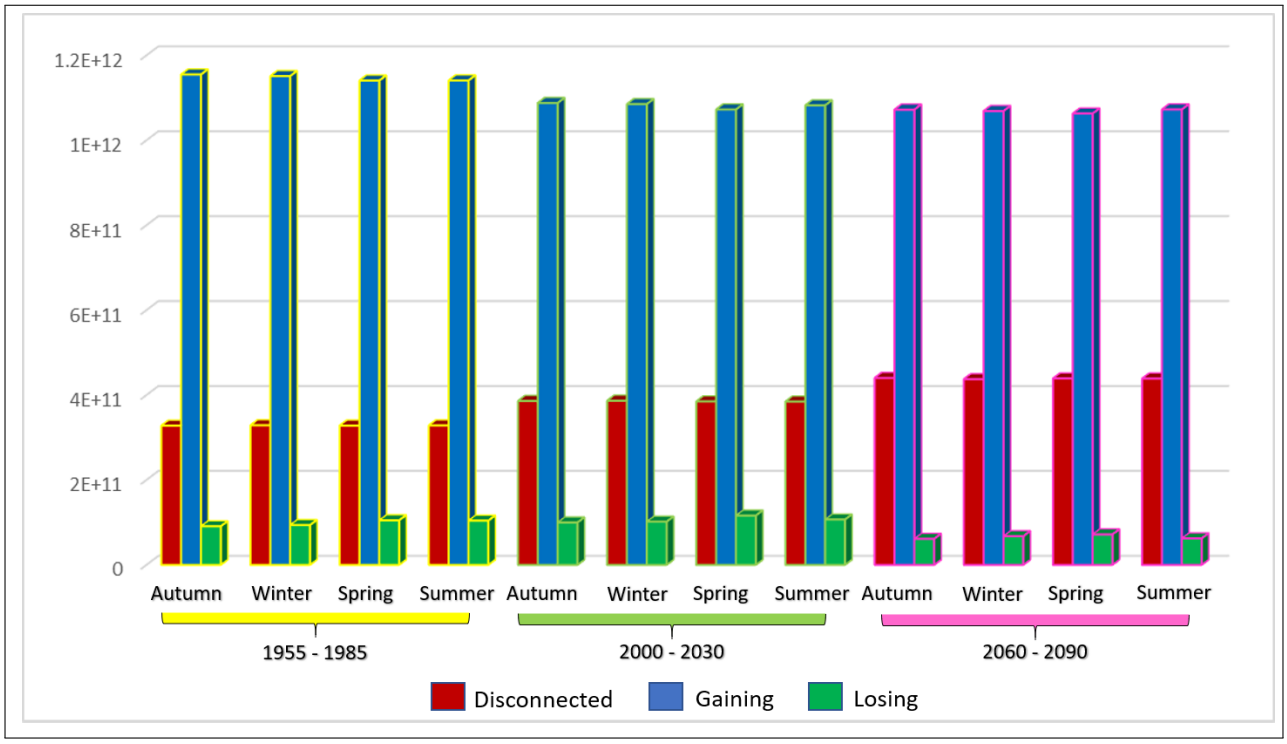

Figure 18: Averaged area (m^2) over 30 years of gaining, losing and disconnected streams break down into the four seasons and three 30-year periods (1955-1985, 2000-2030, 2030-2060).

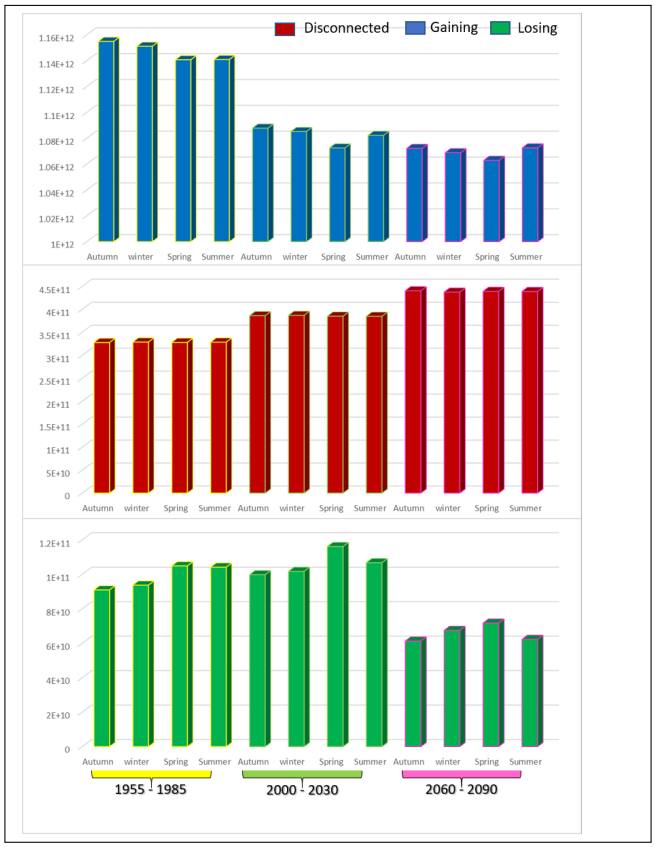

Figure 19: Averaged area (m^2) over 30 years of gaining, losing and disconnected streams break down into the four seasons and three 30-year periods (1955-1985, 2000-2030, 2030-2060).

3.4 GCMs comparison and uncertainties

Three different GCMs were used in order to predict the future interaction between groundwater and streamflow. These three GCMs were chosen because they cover a wet, dry and average scenarios which allows us to know the entire possibility range of changes in groundwater-streamflow interaction for the future. The uncertainty bands were computed according to the variation overlap. This means that the uncertainties computed are not related to the probability that the amount of gaining, losing or disconnected streams will be located in this band but it means that the more the band is large more the variations over a year are large and therefore the harder it is possible to find a water management solution.

As it is visible on figure 12, the area of gaining streams stayed the biggest and the area of intermittently disconnected streams stayed the lowest by far when comparing with the other types of streams. The area of continuously disconnected streams and losing streams are almost the same size but the continuously disconnected streams are always a little bigger.

On figures 12 and 20 we can see that for the gaining streams, the GFDL forcing predicts 13% of area increase. The MIROC forcing only shows an increase of 4.5 % and HadGEM shows a decrease of 9.5 %. The best case scenario is showed by GFDL and the worst is the HadGEM scenario. In figure 20 the uncertainties for each scenario are highlighted. We can see that the HadGEM GCM is the one that shows the highest uncertainty from beginning to end and that it increases with time. The GFDL GCM shows the minimum uncertainty between the three scenarios and with more uncertainties at the beginning than at the end. The uncertainties for the MIROC GCM increases a little over time.

For the area of losing streams, the HadGEM scenario shows an increase of 25% which makes it the worst scenario whereas the two other GCM's show a decrease, of 15% for GFDL and 11% for MIROC. The HadGEM projection is again the one showing the larger uncertainties and these uncertainties are increasing over time. GFDL scenario again shows bigger uncertainties at the beginning than at the end. For the MIROC GCM the uncertainties slowly increase over time.

For the area of intermittently disconnected streams there is an increase of 91% and of 35% for the HadGEM and MIROC projection respectively whereas the GFDL projection shows a decrease of 5%. The uncertainty

for HadGEM scenario is growing overtime and at the end is the one showing the largest uncertainty. The uncertainty for MIROC is growing over time too but in a less striking way than for HadGEM. For GFDL the uncertainty stays constant overtime.

For the area of continuously disconnected streams there is an increase of 4% and of 0.2% for HadGEM and MIROC respectively, whereas there is a decrease of 16% for GFDL. The uncertainty bounds are very small because of the fact that it has to be 2-years in the same state to be considered as continuously disconnected so the variations over time are very small. For the 3 scenarios the uncertainty decrease over time. The GFDL is the scenario with the most uncertainty, MIROC and HadGEM show more or less a similar area of uncertainty.

Figure 20 is a little misleading in the sens that the scale of the graph for each state of stream differs. Table 6 is more helpful to know the probability range of area of gaining, losing, disconnected streams in the future. Looking at these three GCM it is clear that MIROC and GFDL show a more similar future than HadGEM GCM.

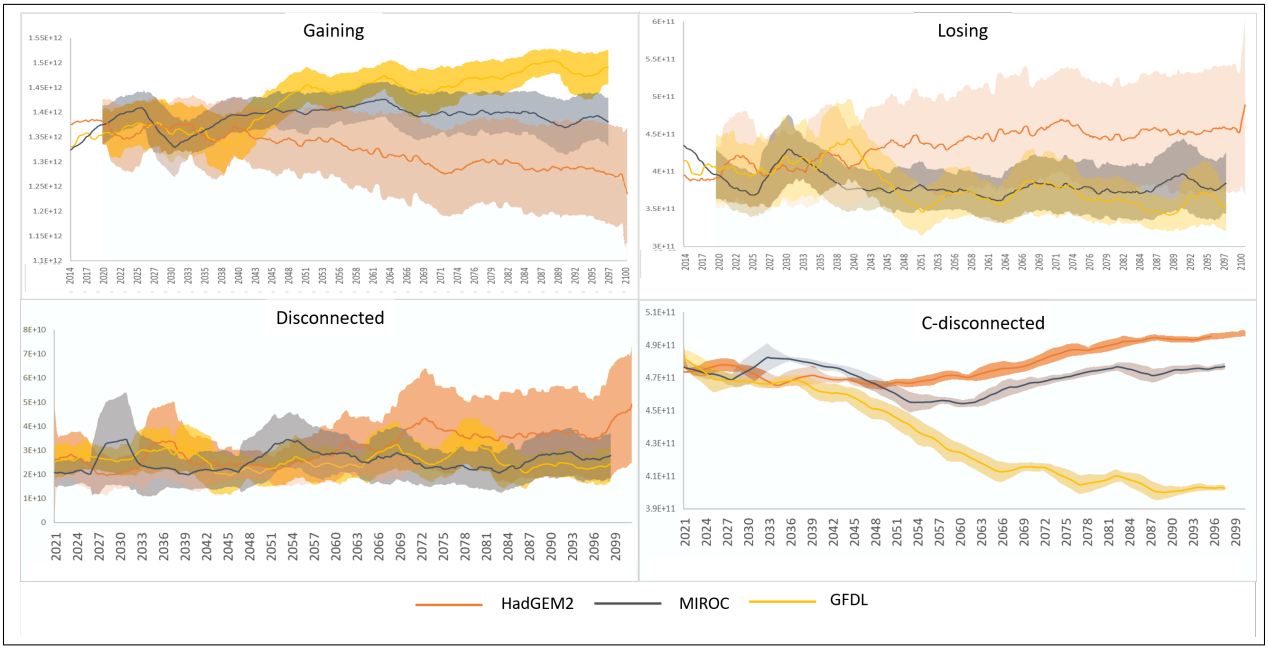

Figure 20: Uncertainty linked to each future scenario: HadGEM (orange), GFDL (yellow), MIROC (grey) for each state of stream (gaining, losing, intermittently disconnected and continuously disconnected). Scale is different for each state of stream on the graph.

Table 6: Percentage of change between 2010 and 2099 for each GCM

Run Name	Percentage of change Gaining streams	Percentage of change Losing streams	Percentage of change intermittently disconnected S.	Percentage of change continuously disconnected S.
HadGEM	-9.5%	25%	91%	4%
GFDL	13%	-15%	-5%	0.2%
MIROC	4.5%	-11%	35%	-16%

3.5 World

This section was made in order to have an insight on what is the model results for the evolution in groundwater-streamflow interaction over the world for the period 1901 to 2010. This run was run with the same forcing data as the Non-Natural run from Edwin.

As we can see on figures 21, the area of gaining streams continuously increases for all stream orders, lower the stream order, sharper is the increase. Only for streams of order 9 that the area of gaining streams decreases. It is visible on figure 22 that the area of gaining streams globally increases over time. The area of gaining streams increases, between 1905 and 1955, are mainly in the North-East part of South-America, in the part just in the South of Sahara, mainly the south of Chad and Cameroon, we can also notice the increase of gaining streams area in the centre of India and finally in the East of Russia. But we can also see a decrease in the amount of gaining streams between June 1905 and June 1955 in the centre of the US (Nebraska), in Paraguay and the state of Brazil at the border of Paraguay, in the North east part of Russia and in the North of Kazakhstan. In between June 1955 and June 2005 the area of gaining streams increases in the centre of US (Nebraska), in Brazil, in the North East part of Russia and in North of Kazakhstan. The area of gaining streams decreases in Africa more precisely in Congo and North of Democratic Republic of Congo.

The area of losing streams globally decreases for all the stream orders except for the streams of order 7 and 9 for which we can notice a slight increase. The area of the world with an obvious increase of area of losing stream are the same as the one with an obvious decrease of gaining streams and the same for area with an evident decrease of losing streams.

The area of intermittently disconnected streams globally decreases for all stream orders. The area of intermittently disconnected streams is small so the changes are not obvious on figure 22. The biggest decrease happened between 1905 and 1955 and are located mainly around Alberta in Canada and in Democratic Republic of Congo. The majority of increases in area of intermittently disconnected streams are situated in South America in Brazil and Argentina. An increase can be seen in South-Africa more precisely in the very south of Democratic Republic of Congo and in Zambia. Between June 1955 and June 2005 the changes are very sparse, there is a small cluster of a decrease of disconnected streams around the border of Kazakhstan and Russia. There is a small cluster of an increase of disconnected streams in the North-West of India.

The area of continuously disconnected streams decreases for streams of order 5, 8 and 9. For streams of order 3, 4 and 6 there is first an increase followed by a decrease. On figure 22 we can see that between 1905 and 1955 there is a large increase of continuously disconnected streams in all of Canada and in the west of the rest of North-America. It is a little spread but there is an increase of continuously disconnected streams in more or less all Asia except from Russia and Thailand and the surrounding countries of Thailand. We can also notice an increase in the East and really south of South-Africa and in Australia. A decrease of continuously disconnected streams can be noticed mainly in Africa, more precisely in Democratic Republic of Congo, Congo and east of Angola. The decrease in area of continuously disconnected streams is also diversely spread but there are less of them than increasing streams. Between 1955 and 2005 the decrease of continuously disconnected streams is more important than the increase, the changes are still sparse though, which make it difficult to point an area. The only area with a clear cluster of change is around the border between India and Pakistan where you can see more continuously disconnected streams and at the border between Washington and Canada where there is a decrease of continuously disconnected streams.

Figure 21: Moving average over 5 years of area in m^2 minus the mean from 1901 to 2010 of gaining, losing, disconnected and continuously disconnected (C-disconnected) stream breaking down into six stream order (3 to 9) (data from Edwin) for the world

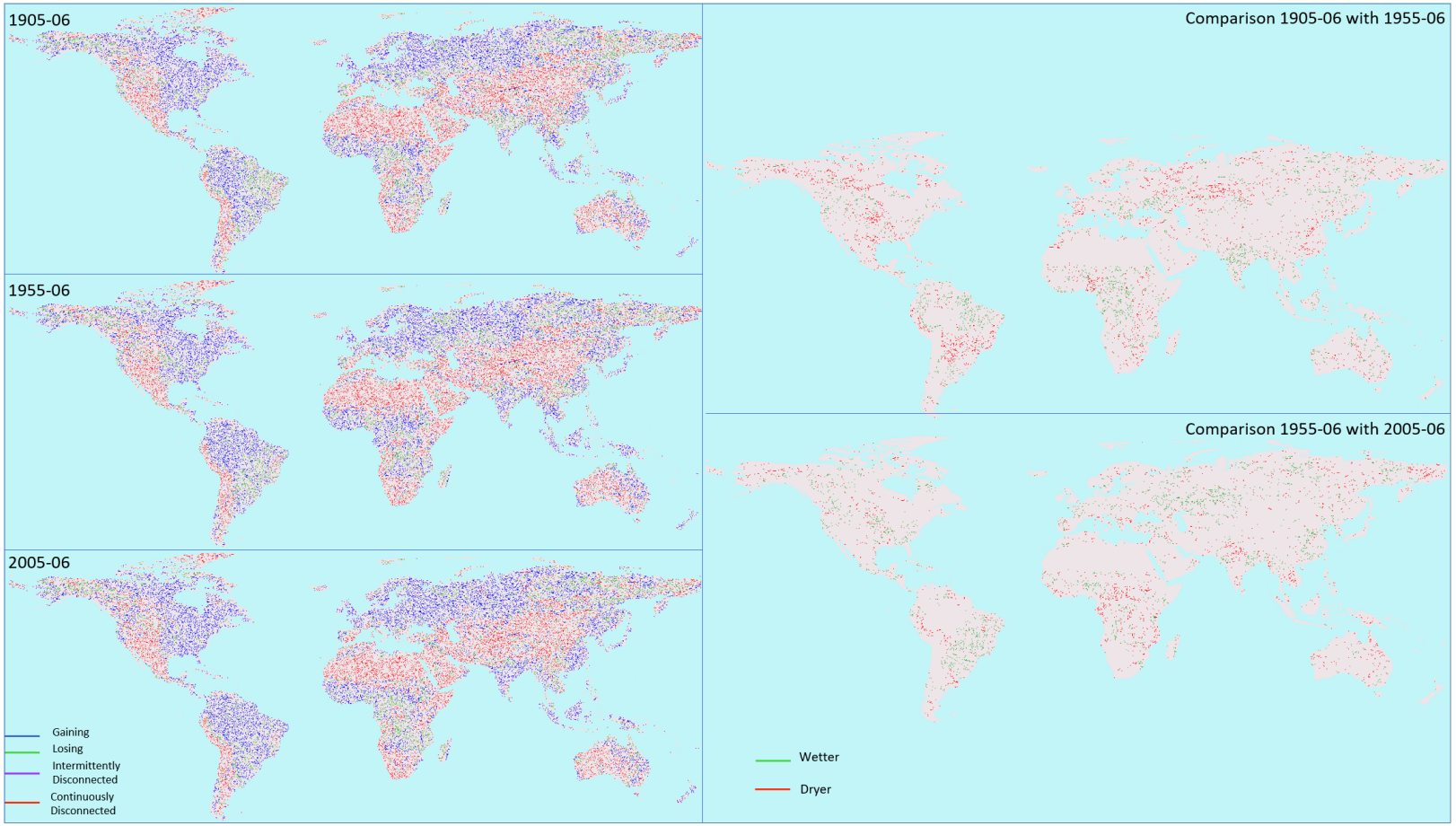

Figure 22: Evolution of the states of streams over time for the historic non-natural run for first column : June 1905, June 1955 and June 2005. The second column shows a changes to wetter (green) or drier(red) stream from June-1905 to June-1955 and from June-1955 to June-2005 for the world

4 Discussion

This research has the purpose to analyse the evolution of groundwater-streamflow interactions over time and space in order to know where and when these changes occurred but also where and when they are likely to occur according to different scenarios. Taking the results from this, we can assess which areas are most at risk of lacking water in the future and support it with logical reasoning as to why these areas may lack water in the future. All of the three projections analysed predict a different scenario for the future availability of water. These differences will be compared and discussed. The human influences on theses changes between groundwater and surface water interaction is also raised. The changes of streams according to their stream orders for the different scenarios is also analysed and explained.

4.1 Validation of the model

The surface water discharge and the groundwater level simulated with PCRGLOBWB coupled with MODFLOW were validated against observations from gauging and well stations in the Upper Arkansas catchment. Overall the simulated discharge shows a better correlation with the observed ones than the simulated groundwater level, because none of them show a negative correlation coefficient and fewer of them have a determination coefficient lower than 0.1.

The poorer groundwater level validation can be explained by the fact that for the groundwater level, it was difficult to compare exactly the same information. Indeed the groundwater level observation is only a punctual observation for which the value strongly depends on the elevation of the piezometer location whereas the simulated groundwater level is an average over a 5 arcmin cell which at the equator would be equivalent to 100 km^2. The amount of variation depends also if the aquifer is confined or unconfined. It may also be possible that PCRGLOBWB underestimates the groundwater recharge. Also for the simulated groundwater level, there is data available for every month in a year whereas for the groundwater level observation there were usually only four observations a year. Despite having less data for the observation than for the simulation, the observed time series still show more variations than the simulated ones for almost all the well stations. Even if the absolute value is not well represented, the trends are approximately similar for almost half of the time series. This means that the baseflow behaviour is timed up well for these time series. In order not to compare a punctual observation with a 100 km^2 area, a baseflow analyses and comparison with observed head could be done in further research.

The coefficient determination are sufficient for the surface water discharge but not good. Indeed the maximum determination coefficient is only 0.436 and there are still 6 gauging stations with a determination coefficient lower than 0.1. The simulated surface discharge water appears to be an overestimation of the real surface water discharge. This might be the result of an overestimation of precipitation and underestimation of evaporation , Beek (van) and Bierkens, 2009, future research would be needed in order to compare simulated precipitation and evaporation with observations. In the paper of Sutanudjaja et. al (2018) they also validated the simulated surface water discharge for 3597 stations over the world from the PRGLOBWB coupled with MODFLOW model and their results are far better. The version of PCRGLOBWB used in this research was a development version of the one used in Sutanudjaja et. al (2018) paper.

It is also important to notice that the observations from the gauging and well stations of USGS are not exempt of error sources either.

To conclude this section, the validation of the model by comparing observed with simulated groundwater level and discharge shows that the quality of the groundwater model is poor. However it seems that the trends of the compared variables are more or less 50% of the time well represented. This means that the absolute values show in the result section are likely to be wrong, but the relative comparison between GCMs and scenarios might still hold. The quality of the groundwater model is difficult to assess as there is little observation data available. Also the scale at which these data are available is different from the model scale.

4.2 Changes in groundwater-streamflow interactions in the past and comparisons with natural conditions for North-America

The model was run for two different historical non-natural scenarios and one historical natural scenario. The two Non-natural scenarios were run with different forcing data. Globally they show the same areas of changes but the extent and rate of changes are different. These three runs show an evolution toward a wetter North-America. The historic period of the reference run was also analysed and compared to these three runs, however it shows a different mask area, different results and was not run with the same version of PCRGLOBWB than the others which make it really difficult to be compared with the other runs.

Comparison of the two non-natural runs

When comparing the two Non-natural run, one can see that the rate of increase in area of gaining streams is more than twice steeper for Edwin's run than for Inge's run. Inge's run shows an increase of 10^5 m^2/month of continuously disconnected streams whereas Edwin's run shows a decrease at the same rate. However, Edwin's run shows an increase in intermittently disconnected streams whereas Inge's run displays a decrease. Therefore, these two runs, even though they were computed with a different set of forcing data, they can be considered as similar as they show almost the same areas of changes and trends. The reference run shows an increase in both types of disconnected streams and a decrease in area of gaining streams that is at the same rate that the increase in continuously disconnected streams which shows an evolution toward a drier North-America contrary to the three other runs.

Comparison of the two non-natural runs with the natural run

When comparing the Non-natural runs with the Natural run, one can see that the increase in gaining streams in the Natural run is the smoothest of the three. This can easily been explained by the fact that it is the scenarios with the biggest amount of gaining streams, therefore, there are less streams available to be changed into gaining streams. The Natural run shows a decrease in all other states of streams, which means that this run simulates a continuous increase in precipitation. Both of the Non-natural runs show a decrease in one of the two disconnected stream states. This can be explained by an increase in groundwater extraction over the years. These increase in disconnected streams are one order of magnitude below the increase in gaining streams. There are two ways to explain the fact that there is more losing streams in the Natural and Non-natural run from Inge than in the non-natural run from Edwin. It could be because a part of the intermittently disconnected streams and continuously disconnected streams in the non-natural run are in the losing state in Inge's runs. It could also only be a question of forcing data that are the same for Inge's runs and different for Edwin's Non-natural run. Indeed, the historic non-natural run from Inge has less losing streams than the natural run which would be expected. Although the historic natural run and the historic non-natural run from Inge show almost the same amount of continuously disconnected streams which could only be explained by the fact that the streams are staying longer in a losing state before turning into disconnected streams for the non-natural run of Inge. This means that the forcing data of Inge (ERA-Interim) show a less enhance global warming, than the forcing data from Edwin (ERA-20C) as suggested by Poli et. al (2013 and 2016).

Areas of change for the three historical scenarios

As North-America is split into a dry part (West) and a wet part (East). The expectation was that it becomes drier at the intersection of the wet and the dry part. This fragmentation can be easily explained with the topography and the climate. The relief of the west part is a high relief characterised by the Rocky mountains. In the middle of the continent there is the Great Plains, for which the topography is lower than for the Western part but higher than for the eastern part that is quite smooth and low. As it is higher and drier in the Western part of the continent, the groundwater tables are deep which lead to continuously disconnected states of streams. On the eastern part, the lower relief allows interaction between groundwater and surface water.

For the three runs, one can see that it is mostly the north part of the US Great Plains that becomes drier. The climate there is continental which means low humidity and precipitation, irrigation for the cultivation is thus needed and as there is not much recharge, this can lead to depletion. The irrigation return flow does not recharge the aquifer for most of the area due to the deep groundwater table (Scanlon et al. , 2010). However it is also becoming drier there for the Natural run but at a smaller extent as Nebraska is not becoming drier in the natural run. The fact that the north part of the US Great Plain also becomes drier in the natural run, means that the principal cause is climate driven and not human driven. The areas around the border between Guatemala and Mexico tend to be drier in these three runs too. This could be because of a weaker monsoon as it is in a monsoonal region. The north-west of the US and south-west of Canada become wetter, this could be explained by more return flow from irrigation (Konikow and Leake , 2014) but again, even if at a smaller extent, it is the case for the natural run too so it can not only be because of return flow from irrigation, this could also be explained by the fact that precipitation has increased from 5 to 30% in southern Canada from 1900 to 1998 (Zhang et al. , 2000). The tributaries of the Missouri river also become wetter in Missouri and Arkansas states which could be due partly to return flow but also to more precipitation. The Missouri river in the contrary becomes drier. Most of the streams in Texas are drier for the Natural and Non-natural run of Inge but wetter for the Non-natural run of Edwin. One of the hypothesis can be that the changes are due to the sea level rise, happening because of climate warming and the subsidence of the coast of Texas caused by groundwater extraction (Paine , 1993).

It is interesting to notice that most of the changes occur in the Natural and Non-natural runs. Sometime at a smaller extent in the Natural run. The fact that in figure 10, the maps for the Non-natural runs and the Natural run are similar means that climate influence has a bigger impact on groundwater streamflow interaction than human influence. This funding is in contradiction with what Taylor said :" *The indirect effect of climate on groundwater through changes in irrigation demand and sources can be greater than the direct impacts of climate on recharge.*" (Taylor et al. , 2013). In this research, it is more correct to say that the impact of human on the climate lead to more extreme changes on groundwater-streamflow interaction than the direct extraction of groundwater.

Comparison between the areas of change for the historical period of the reference run and the three other historical runs

The reference run shows more drier streams than the Natural run and the Non-natural runs. The drier streams seems to spread from west to east and the Great Plains are becoming drier and drier when looking at figure 10. Only an area of drier streams in Nebraska are similar to the two Non-Natural runs. The drier streams should mainly be due to climate as there are not in the Edwin non-natural run which the reference run was calibrated with, and the HadGEM GCM only takes into account climate changes. Although it was calibrated with the Edwin's Non natural run, it does not mean that the two runs will show the same trend, they will just have a similar mean and variation. However, the variations are not similar either because the reference run was run with a different version of PCRGLOBWB that mitigates the variation, as the groundwater storage was considered to change too abruptly in the previous version. The means are not comparable as the mask area is not the same.

Future research

For further research, a climatology on every historic run should be done in order not to compare a single month with another single month, but a 30-year period with a 30-year period. The maps would be more relevant to compare with each other. It would also be interesting to see if where there are changes, is it due to a change in groundwater head or a change in river head? It is not so straightforward as there are a lot of variations over time in those variables. It would also be interesting to run the Non-natural run from Edwin with the same version of PCRGLOBWB as the one used for the reference run in order to make them more comparable with each other.

4.3 Changes in groundwater-streamflow interactions in the past for the World

A quick analysis of groundwater-streamflow interaction was made for the world in order to see if a pattern could be distinguished. Indeed, many studies show or predict that wet areas are becoming wetter and dry areas are becoming drier (Lu et al. , 2007, Allan et al. , 2014, Putnam and Broecker , 2017), this is not something that we can see on figure 22. Instead, we can see that what is becoming dry or wet in the first half of the last century can change in the opposite way in the second half of the century. However, it is important to notice that this observation is only based on the comparison of a single month with another single month 50 years after. Even though this comparison is not significant enough to draw conclusions, here follows an explanation for the changes that are visible on figure 22.

Figure 22 shows that the part of the world that was already dry in 1905 was the western part of America. The Sahara in the North, Ethiopia and Somalia in the east and the very south of Africa, the most part of Australia, extreme east of Siberia and finally the south part (but not the extreme south) and the west part of Asia. Therefore, it is at the border of these locations that changes are expected. All these regions are classified as arid or semi-arid climate area according to the Köppen–Geiger classification (Kottek et al. , 2006).

Indeed there are always changes happening around these areas but when looking carefully changes are happening everywhere except at the very location of these arid areas (and lakes). There is not a clear pattern coming from figure 22, meaning that around the arid areas previously cited, it is not always becoming wetter or drier, it changes according to the location of the arid area and the period. The reasons of these changes can be due to climatic changes such as stronger or weaker monsoons if in monsoonal regions (Huang et al. , 2016), or by enhanced or diminished westerlies if in between 30-60° latitude (Huang et al. , 2016). These changes can also be caused by human influences such as more groundwater extraction that can also lead to more return flow from irrigation. Increase in groundwater extraction can be due to an increasing population and economical development.

4.4 Changes in groundwater and surface water interactions in North-America for the future scenarios

The model was run for three different GCMs that are HadGEM, GFDL and MIROC under the 8.5 RCP that represent an average, dry and wet scenario respectively. The areas of change for each of these GCMs are globally the same but not the trends. A part of the reference run was run for the future with the HadGEM GCM and surprisingly shows different areas of change. The results of these three GCMs enable an estimation of the probability bands in which the amount area of gaining, losing, intermittently and continuously disconnected streams will be in the future. Recall that for the three GCMs a "business-as-usual" scenario was assumed which means that only climate changes are taken into account.

Trends and areas of change for the future projections

The first striking fact when looking at figure 12 is that the the HadGEM GCM, that should be the average projection, turns out to be the dry projection, GFDL that should be the dry projection, turn into being the wet projection and MIROC that is the wet projection, becomes the average projection. This is due to the fact that thoses GCMs are for the world. For the wet projection only some parts of the world are becoming wetter and for the dry projection only some parts of the world are becoming drier. It is apparently not the parts that are analysed in this study.

When looking at figure 13, one can see that for the GFDL GCM, North-America tends to be wetter and wetter, mainly in south-west of Canada and north west of the US. Texas tends to be drier. This is confirmed with table 4 that shows an increase in gaining streams area and a decrease in all other types of streams. The trends of the HadGEM GCM are clearly toward drier states of streams over time with a clear increase in losing, intermittently and continuously disconnected streams and a large decrease in gaining streams as shown in table 4. Streams are becoming drier in the west and south of the map, so in Canada and north-west of the US. The reference run shows an increase in drier streams for the first half of the century and almost none afterwards. The area of increase in drier streams for the HadGEM run is not represented on the reference run, so it is difficult to say if the results are similar. However, the area of increases in drier streams for the reference run are located in the south of the Great Plains and in the north of Mexico which is the case in none of the other future projections. It also shows that in North Dakota and North of Nebraska the area is becoming wetter and wetter. There are a lot of variations in the MIROC GCM, a continuous trend is not visible. It looks like the first half of this century is going toward a wetter state of streams and is similar to GFDL results whereas the second half is evolving toward a drier state of streams and is similar to HadGEM result. On table 4, the global trend of MIROC is still toward a wetter state because of the increase in gaining streams and decrease in continuously disconnected streams.

As a "business-as-usual" scenario was assumed the areas of changes that are located around the Rocky Mountains, could be due to a change in eternal snow melt or, and this is true for every other areas of change, more or less precipitations. If an increase in water demand over time was taking into account, which is very likely as the population is growing as well as the economy, it is possible that the GFDL and MIROC scenarios would tend toward a drier state of streams in the future.

Uncertainty analysis

An analysis on the amplitude of variation of each state of stream for each GCM was done, as well as a comparison of the percentage of changes (done on the moving average) between 2010 and 2099. Table 6 shows that in our predictions a large probability bands of changes in states of streams is conceivable. Indeed, the areas of gaining streams can change from -9.5 to +4.5%, the area of losing streams from -15% to +25%, the area of intermittently disconnected streams from -5% to +91% and finally the area of continuously disconnected streams from -16% to +4%.

As we can see on figure 20, HadGEM is the GCM showing the largest amplitude of variation and it increases over time, whereas MIROC and GFDL shows more or less the same overlap area, this area even decreases slightly for GFDL and increase a subtle amount for MIROC. The fact that the magnitude of variation decreases over time for GFDL could be meaning that when a stream is in a certain state for a while it is likely to stay in this state of stream. What can be concluded from this analysis is that if HadGEM predicts correctly, it will be hard in the future to establish a stream management policy, as the groundwater and surface water recharge will vary a lot between seasons. However, in the reference run computed with a new version of PCRGLOBWB, these variations are largely restricted. It would then, be interesting to compute a "reference run" with the MIROC and GFDL GCMs in order to compare them. Then, the one showing the most similarity with the historic non-natural run, would be the likeliest to happen. However, looking at these three GCMs, one can

conclude that there are 2/3 chance that in the future it will be like MIROC and GFDL prediction than like HadGEM prediction for North-America but there is still 1/3 chance that it will be as HadGEM predicts.

For the three scenarios, the area of overlap for the continuously disconnected state of stream is decreasing over time. This can support the idea that when a stream becomes continuously disconnected, the groundwater table continues depleting at a faster rate (fig.2) whereas the infiltration of water from the river reaches a maximum rate and can not be faster.

This analysis shows that it is important to use more than one GCM in order to make projections in evolution of interaction between groundwater and surface water as the results are very different depending on which GCM is used because the model is very sensitive to the different GCMs. It would be interesting to compare 30-year periods between GCMs in order to make a more meaningful analysis of where the changes are likely to happen.

4.5 30-year periods analysis of groundwater-streamflow interaction in North-America

Because of the distinction between intermittently and continuously disconnected streams, the areas of changes were determined by comparing a month with a month which really weakens the significance of the analyses in this study. Therefore a 30-years period with another 30-years period comparison was done for one of the run. The run that was chosen was the reference run as it has continuous information for the past and the future. First the areas of changes are compared and explained and then the trends are explained by period and by seasons. The influence of streams order is also analysed but then for all the runs.

Areas of change

On figures 16 and 17, we can see that the areas becoming drier between the first and the second period continue getting drier between the second and third period. The same is true with the wet areas that keep getting wetter. This is something that one could already see in figures 10 and 13 that compare a month with another month. The fact that a 30-year period is compared with another 30-year periods makes the result more relevant. This result, contrary to what was said in section 4.3, agreed with the statement that dry areas get drier and wet areas get wetter (Lu et al. , 2007, Allan et al. , 2014, Putnam and Broecker , 2017). It is important to notice that it is only a small area, it is not sufficient to prove that this statement is true for all regions in the world. Again, as on figures 10 and 13, we can see that most of the west and north-west areas are getting drier except for the area around the border between South-Dakota and Nebraska, where the streams are getting wetter. This matches our expectations of seeing changes at the transition between the wet and the dry part of the US. It is good to note that the 30-years period comparison gives the same results as the 1-month period comparison. Although this one observation is not sufficient to say that it would be true for every scenario.

Trends in each types of stream over time and between seasons

On figures 18 and 19 one can see clearly that there is a decrease of gaining streams and an increase of disconnected streams over time. The area of losing streams first increases slightly between the first and second 30-year period and after decreases a large amount between the second and the third period. The major decrease of gaining streams happens between the first and the second 30-year periods. Therefore it can be assumed that between the first and the second 30-year periods, the gaining streams turn into losing and disconnected streams and between the second and the third periods, it is mainly the losing streams that turn into disconnected streams. This shows again that for the reference run the streams are becoming drier and drier. Figure 19 shows that for the area of gaining and losing streams, the seasons have an influence, but not for the disconnected streams. Although, it is counter-intuitive that spring is the season with the most losing streams and the least gaining streams for the second and third 30-year periods.

Influences of stream orders

In this study a thorough analysis was made on the different behaviours between streams depending on their order. It would be expected that the streams of low order (3, 4, 5) act as the opposite of the streams of higher order (7, 8). This is because the groundwater pumping affects streams of higher order and return flow first affects streams of lower order. When the groundwater is too deep the return flow does not influence the interaction between groundwater and surface water anymore. It is noticeable that the groundwater pumping does not directly affect the streams, there is a time delay between the groundwater pumping and the effect on streams. At the same time, streams of lower order could be more sensitive to groundwater extraction than

streams of higher order due to the fact that their discharges are lower. Lower stream orders will also be more sensitive to the lithology of the subsurface.

Although the results tend to show that the order of streams show a different behaviour only for the Natural and Non-natural run of Inge. Indeed, for these runs, streams of order 3 and 4 act in the opposite way to streams of order 5 and 7. For the Non-natural run of Edwin, the GCM runs and the reference run the streams act the same way for each order. The lower orders are usually more sensitive and show sharper trends, this can easily be explained by the fact that there are far more of them than the higher order of streams. The effect of groundwater extraction on stream orders should be done on a small single catchment for which the lithology of the subsurface is known and is the same for different stream orders of this very catchment.

5 Conclusion

To conclude the PCR-GLOBWB model does not simulate well the absolute value but the timing of surface water and groundwater recharge is simulated in a satisfactory enough way for the aims of this study. There is now a better version (Sutanudjaja et al. , 2018) that is proved to be more accurate.

When looking at the historical period it appears that North-America becomes wetter over time. Mainly in north west of the US and in the Missouri, Arkansas states. However, the north part of the US Great Plain seems to become drier, as well as the Missouri river, and areas around the border of Mexico and Guatemala. Most of these changes can be seen in the Natural run too, which lead to the conclusion that most of the visible changes aroused from climate change and humans only have a small impact on them. However some drier areas as the Mississippi river, Texas and Nebraska states seems to be the result of human influences such as groundwater extraction for irrigation.

Three projections for assessing the evolutions of groundwater-streamflow interaction until the end of our century were performed. These projections used three GCM: HadGEM, MIROC and GFDL. MIROC and GFDL shows that North-America tends toward becoming wetter, whereas HadGEM shows an opposite trend. Which can be read as there is 66.6% chance that North-America becomes wetter and 33.4% chance that it becomes drier. The mains areas that becomes wetter with the GFDL and MIROC GCM are the north-west of the US and the south-west of Canada. These three GCMs show a large range of probability for the future of gaining, losing, intermittently and continuously disconnected streams. Therefore the importance of using many GCMs in order to make projections for the future is shown to be necessary. Each GCM should be calibrated with an historic run and should be run continuously from the past to the future, in order to compare which one has the most similar historic period to the historic observation and then, the most suitable GCM could be determined.

During this research a run from 1950 to 2099 was made with the HadGEM GCM calibrated on the historic period. As the HadGEM GCM this run shows a strong trend toward a drier state of North-America. An analysis on seasonal changes of groundwater-streamflow interaction was done. This analysis shows that the seasonal behavior of streams is and is due to change. Indeed, at the end of the century, it is projected that there will be more gaining streams during summer than during winter.

A small analysis on the world for the historic period was made in this research, but it would be interesting to dig into it more by making an analysis on 30 years period and by analysing for the future too. This analysis shows that changes occur around arid and semi-arid areas but there is not specific trend toward a drier or wetter state of streams.

References

Aeschbach-Hertig, W. and T. Gleeson
2012. Regional strategies for the accelerating global problem of groundwater depletion. *Nature Geoscience*, 5(12):853–861.

Allan, R. P., C. Liu, M. Zahn, D. A. Lavers, E. Koukouvagias, and A. Bodas-Salcedo
2014. Physically Consistent Responses of the Global Atmospheric Hydrological Cycle in Models and Observations. *Surveys in Geophysics*, 35(3):533–552.

Bartolino, J. and W. Cunningham
2003. Ground-Water Depletion Across the Nation. Fact Sheet 103-03, U.S Geological Survey, Virginia.

Beek (van), R. L. and M. F. P. Bierkens
2009. The Global Hydrological Model PCR-GLOBWB: Conceptualization, Parameterization and Verification. Technical report, Department of Physical Geography, Utrecht University, The Netherlands.

Core_Team
2008. R: A Language and Environment for Statistical Computing. Technical report, R Foundation for Statistical Computing, Vienna, Austria. {ISBN} 3-900051-07-0.

Dee, D. P., S. M. Uppala, A. J. Simmons, P. Berrisford, P. Poli, S. Kobayashi, U. Andrae, M. A. Balmaseda, G. Balsamo, P. Bauer, P. Bechtold, A. C. M. Beljaars, L. van de Berg, J. Bidlot, N. Bormann, C. Delsol, R. Dragani, M. Fuentes, A. J. Geer, L. Haimberger, S. B. Healy, H. Hersbach, E. V. Hólm, L. Isaksen, P. Kållberg, M. Köhler, M. Matricardi, A. P. McNally, B. M. Monge-Sanz, J.-J. Morcrette, B.-K. Park, C. Peubey, P. de Rosnay, C. Tavolato, J.-N. Thépaut, and F. Vitart
2011. The ERA-Interim reanalysis: configuration and performance of the data assimilation system. *Quarterly Journal of the Royal Meteorological Society*, 137(656):553–597.

Dhungel, R. and F. Fiedler
2016. Water Balance to Recharge Calculation: Implications for Watershed Management Using Systems Dynamics Approach. *Hydrology*, 3(1):13.

Graaf (de), I. E. M., T. Gleeson, R. L. Beek (van), E. Sutanudjaja, and M. F. P. Bierkens
. Environmental flow limits to global groundwater pumping. *Nature*. Submitted.

Gupta, H. V., H. Kling, K. K. Yilmaz, and G. F. Martinez
2009. Decomposition of the mean squared error and NSE performance criteria: Implications for improving hydrological modelling. *Journal of Hydrology*, 377(1-2):80–91.

Harbaugh, A., E. Banta, M. Hill, and M. McDonald
2000. MODFLOW-2000, The U.S. Geological Survey Modular Ground-Water Model - User Guide to Modularization Concepts and the Ground-Water Flow Process. Open-File Report 2000-92, U.S. Geological Survey.

Hempel, S., K. Frieler, L. Warszawski, J. Schewe, and F. Piontek
2013. A trend-preserving bias correction - the ISI-MIP approach. *Earth System Dynamics Discussions*, 4(1):49–92.

Huang, J., M. Ji, Y. Xie, S. Wang, Y. He, and J. Ran
2016. Global semi-arid climate change over last 60 years. *Climate Dynamics*, 46(3-4):1131–1150.

Karssenberg, D., O. Schmitz, P. Salamon, K. de Jong, and M. F. Bierkens
2010. A software framework for construction of process-based stochastic spatio-temporal models and data assimilation. *Environmental Modelling & Software*, 25(4):489–502.

Konikow, L.
2015. Long-Term Groundwater Depletion in the United States. *Groundwater*, 53(1):2–9.

Konikow, L. and S. Leake
2014. Depletion and Capture: Revisiting "The Source of Water Derived from Wells". *Groundwater*, 52(S1):100–111.

Kottek, M., J. Grieser, C. Beck, B. Rudolf, and F. Rubel
2006. World Map of the Köppen-Geiger climate classification updated. *Meteorologische Zeitschrift*, 15(3):259–263.

Lu, J., G. A. Vecchi, and T. Reichler
2007. Expansion of the Hadley cell under global warming. *Geophysical Research Letters*, 34(6).

Paine, J. G.
1993. Subsidence of the Texas coast: inferences from historical and late Pleistocene sea levels. *Tectonophysics*, 222(3-4):445–458.

Poli, P., H. Hersbach, D. P. Dee, P. Berrisford, A. J. Simmons, F. Vitart, P. Laloyaux, D. G. H. Tan, C. Peubey, J.-N. Thépaut, Y. Trémolet, E. V. Hólm, M. Bonavita, L. Isaksen, and M. Fisher
2016. ERA-20c: An Atmospheric Reanalysis of the Twentieth Century. *Journal of Climate*, 29(11):4083–4097.

Poli, P., H. Hersbach, D. G. H. Tan, D. P. Dee, J.-N. Thépaut, A. Simmons, C. Peubey, P. Laloyaux, T. Komori, P. Berrisford, R. Dragani, Y. Trémolet, E. V. Hólm, M. Bonavita, L. Isaksen, and M. Fisher
2013. The data assimilation system and initial performance evaluation of the ECMWF pilot reanalysis of the 20th-century assimilating surface observations only (ERA-20c). Technical Report 14, ECMWF, Shinfield Park, Reading.

Putnam, A. E. and W. S. Broecker
2017. Human-induced changes in the distribution of rainfall. *Science Advances*, 3(5).

Scanlon, B., R. Reedy, J. Gates, and P. Gowda
2010. Impact of agroecosystems on groundwater resources in the Central High Plains, USA. *Agriculture, Ecosystems & Environment*, 139(4):700–713.

Sophocleous, M.
2002. Interactions between groundwater and surface water: the state of the science. *Hydrogeology Journal*, 10(1):52–67.

Strahler, A. N.
1957. Quantitative analysis of watershed geomorphology. *Transactions, American Geophysical Union*, 38(6):913.

Sutanudjaja, E. H., R. van Beek, N. Wanders, Y. Wada, J. H. C. Bosmans, N. Drost, R. J. van der Ent, I. E. M. de Graaf, J. M. Hoch, K. de Jong, D. Karssenberg, P. López López, S. Peßenteiner, O. Schmitz, M. W. Straatsma, E. Vannametee, D. Wisser, and M. F. P. Bierkens
2018. PCR-GLOBWB 2: a 5 arcmin global hydrological and water resources model. *Geoscientific Model Development*, 11(6):2429–2453.

Taylor, R. G., B. Scanlon, P. Döll, M. Rodell, R. van Beek, Y. Wada, L. Longuevergne, M. Leblanc, J. S. Famiglietti, M. Edmunds, L. Konikow, T. R. Green, J. Chen, M. Taniguchi, M. F. P. Bierkens, A. MacDonald, Y. Fan, R. M. Maxwell, Y. Yechieli, J. J. Gurdak, D. M. Allen, M. Shamsudduha, K. Hiscock, P. J.-F. Yeh, I. Holman, and H. Treidel
2013. Ground water and climate change. *Nature Climate Change*, 3(4):322–329.

Uppala, S. M., P. W. KÅllberg, A. J. Simmons, U. Andrae, V. D. C. Bechtold, M. Fiorino, J. K. Gibson, J. Haseler, A. Hernandez, G. A. Kelly, X. Li, K. Onogi, S. Saarinen, N. Sokka, R. P. Allan, E. Andersson, K. Arpe, M. A. Balmaseda, A. C. M. Beljaars, L. V. D. Berg, J. Bidlot, N. Bormann, S. Caires, F. Chevallier, A. Dethof, M. Dragosavac, M. Fisher, M. Fuentes, S. Hagemann, E. Hólm, B. J. Hoskins, L. Isaksen, P. A. E. M. Janssen, R. Jenne, A. P. Mcnally, J.-F. Mahfouf, J.-J. Morcrette, N. A. Rayner, R. W. Saunders, P. Simon, A. Sterl, K. E. Trenberth, A. Untch, D. Vasiljevic, P. Viterbo, and J. Woollen
2005. The ERA-40 re-analysis. *Quarterly Journal of the Royal Meteorological Society*, 131(612):2961–3012.

Wada, Y., L. P. H. van Beek, and M. F. P. Bierkens
2012. Nonsustainable groundwater sustaining irrigation: A global assessment: Nonsustainable groundwater sustaining irrigation. *Water Resources Research*, 48(6).

Zhang, X., L. A. Vincent, W. Hogg, and A. Niitsoo
2000. Temperature and precipitation trends in Canada during the 20th century. *Atmosphere-Ocean*, 38(3):395–429.

Appendices

A Method

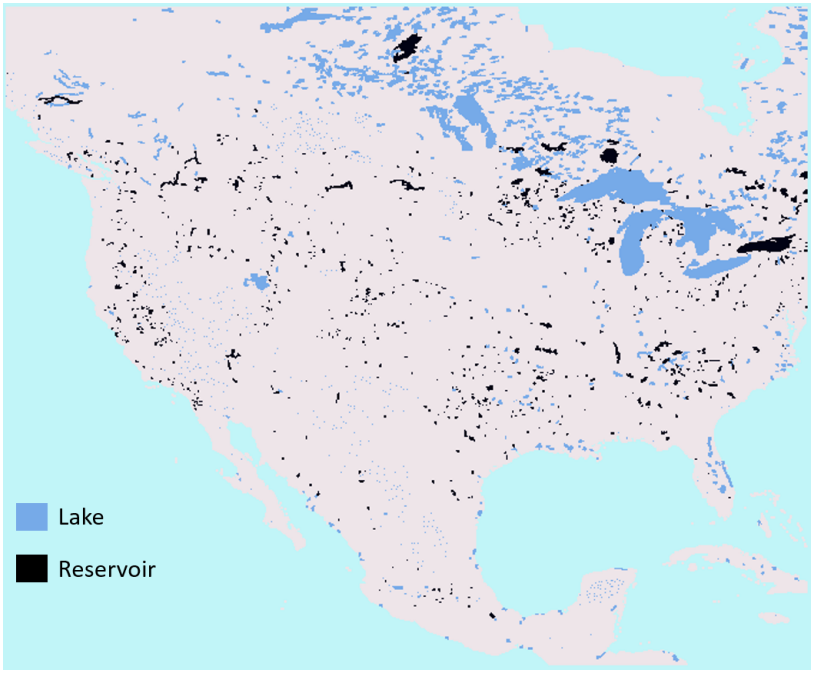

Figure A.1: This map shows the locations of lakes and reservoirs in North-America.

B validation of the model

Surface water discharge

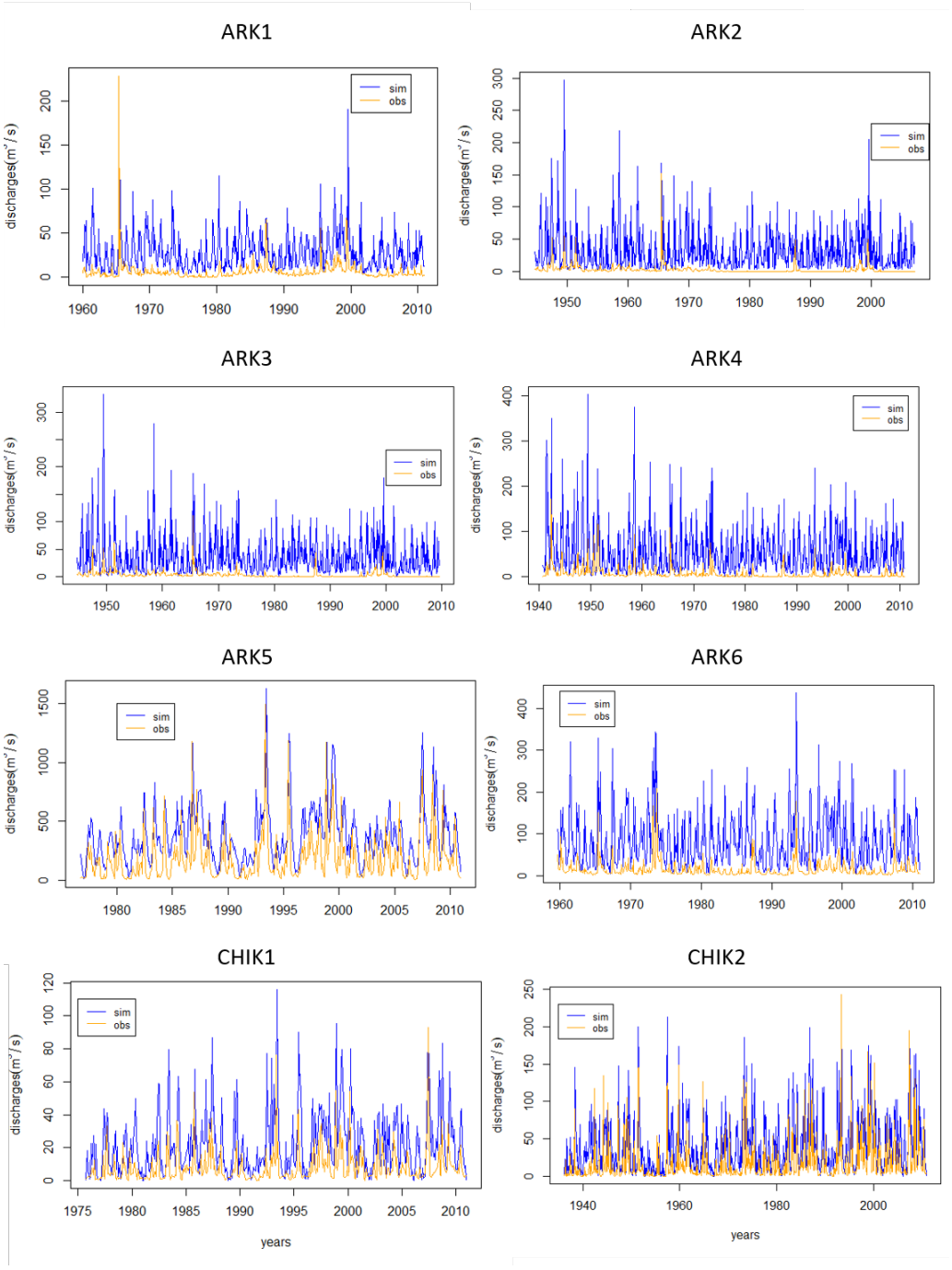

Figure B.1: Time series of observed and simulated surface water discharge for the station ID's : ARK1, ARK2, ARK3, ARK4, ARK5, ARK6, CHIK1 and CHIK2.

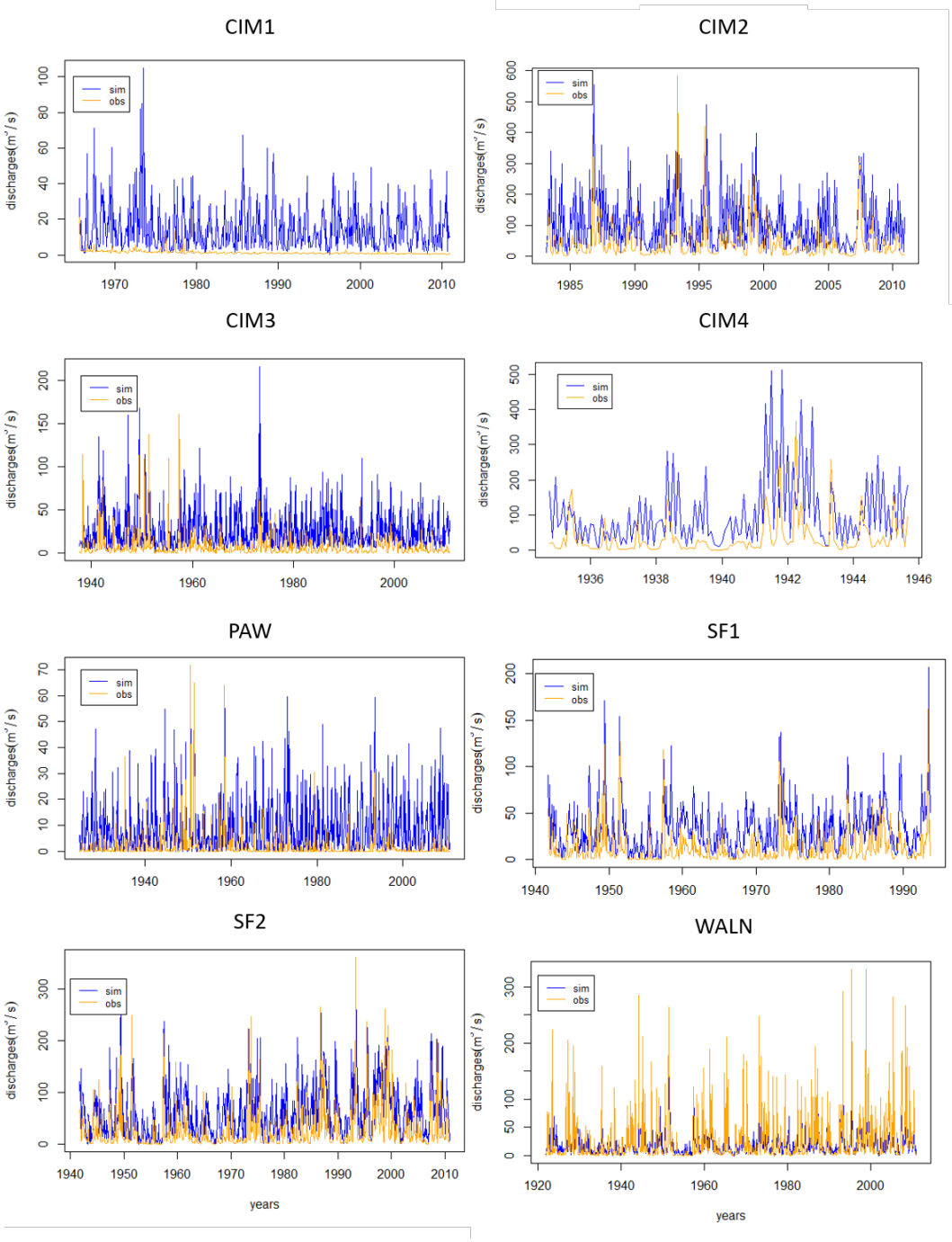

Figure B.2: Time series of observed and simulated surface water discharge for the station ID's : CIM1, CIM2, CIM3, CIM4, PAW, SF1, SF2 and WALN.

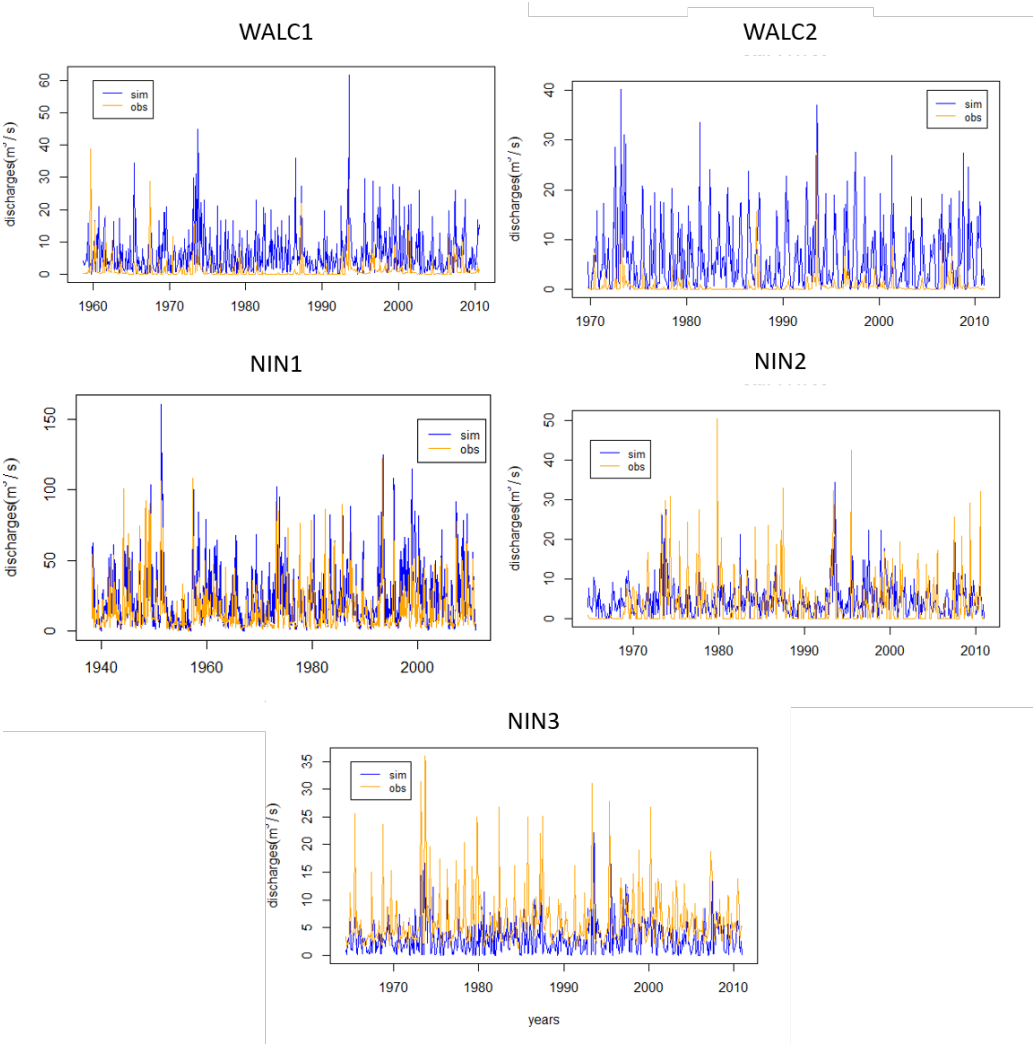

Figure B.3: Time series of observed and simulated surface water discharge for the station ID's : WALC1, WALC2, NIN1, NIN2 and NIN3.

Groundwater level

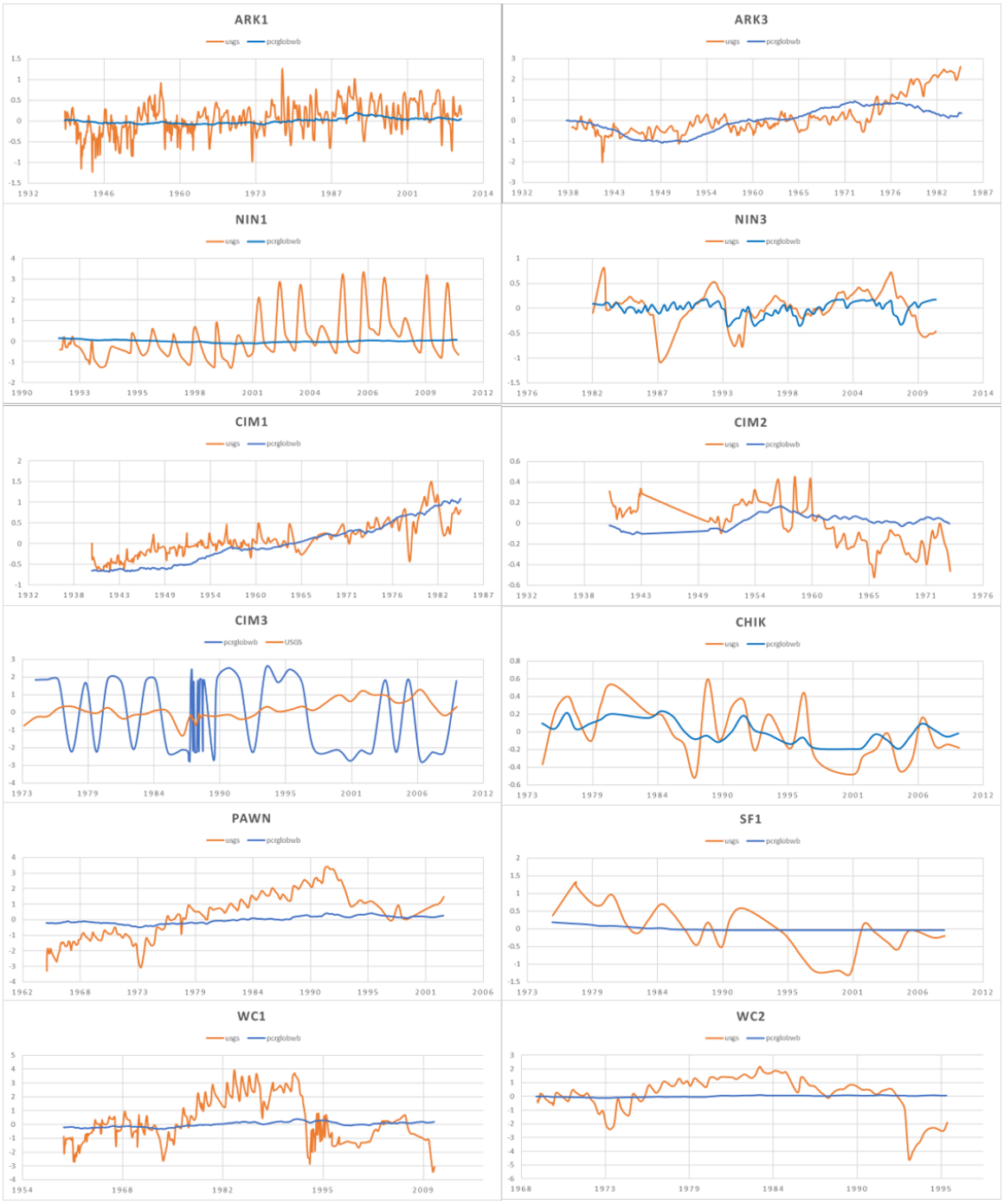

Figure B.4: Time series of observed (orange) and simulated (blue) groundwater level with only the data used for computed the determination coefficient for the station ID's : ARK1, ARK3, NIN1, NIN3, CIM1, CIM2, CIM3, CHIK, PAWN, SF1, WC1 and WC2.

Figure B.5: Time series of observed (orange) and simulated (blue) of groundwater level with only the data used for computed the determination coefficient for the station ID's : WALN, ARK2, ARK4, ARK5, CIM4, CIM5 and NIN2 .

C Groundwater-streamflow interactions

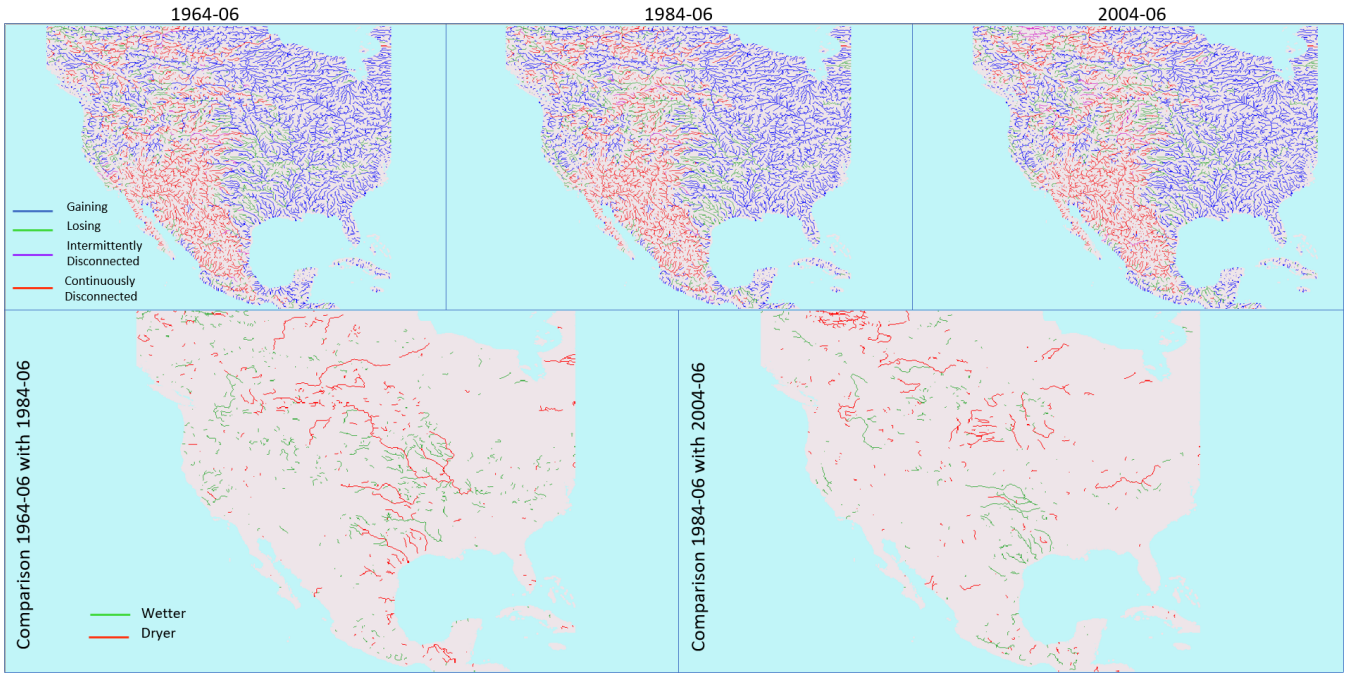

Figure C.1: Evolution of the states of streams over time for the historic natural run for first row: June 1964, June 1984 and June 2004. The second row shows a changes to wetter (green) or drier(red) stream from June-1964 to June-1984 and from June-1984 to June-2004

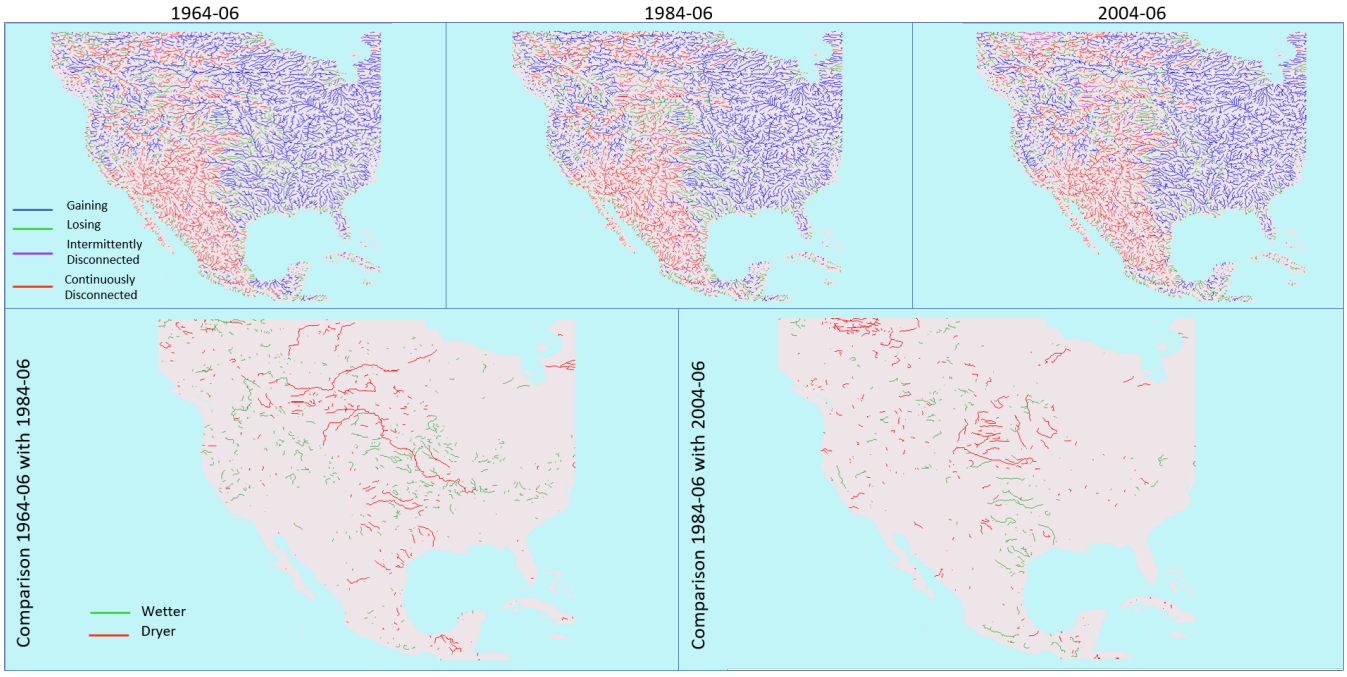

Figure C.2: Evolution of the states of streams over time for the historic non-natural run from Inge for first row: June 1964, June 1984 and June 2004. The second row shows a changes to wetter (green) or drier(red) stream from June-1964 to June-1984 and from June-1984 to June-2004

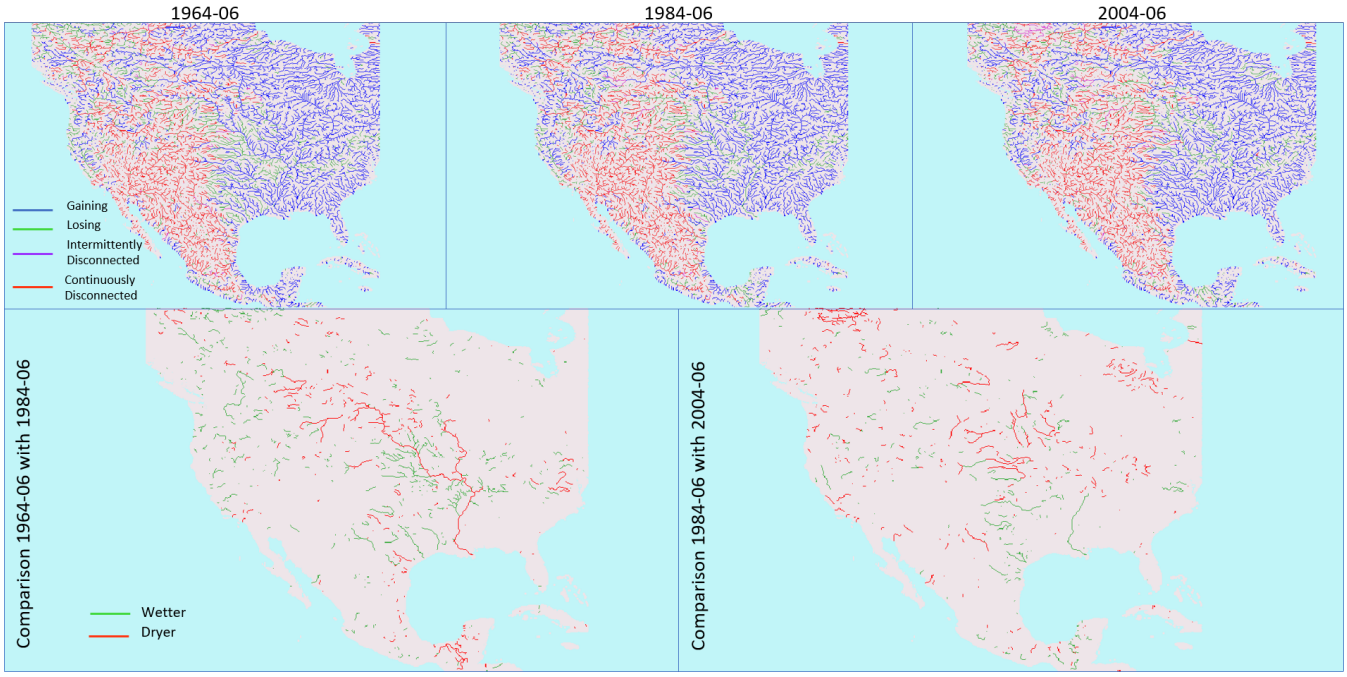

Figure C.3: Evolution of the states of streams over time for the historic non-natural run from Edwin for first row: June 1964, June 1984 and June 2004. The second row shows a change to wetter (green) or drIer(red) stream from June-1964 to June-1984, from June-1984 to June-2004.

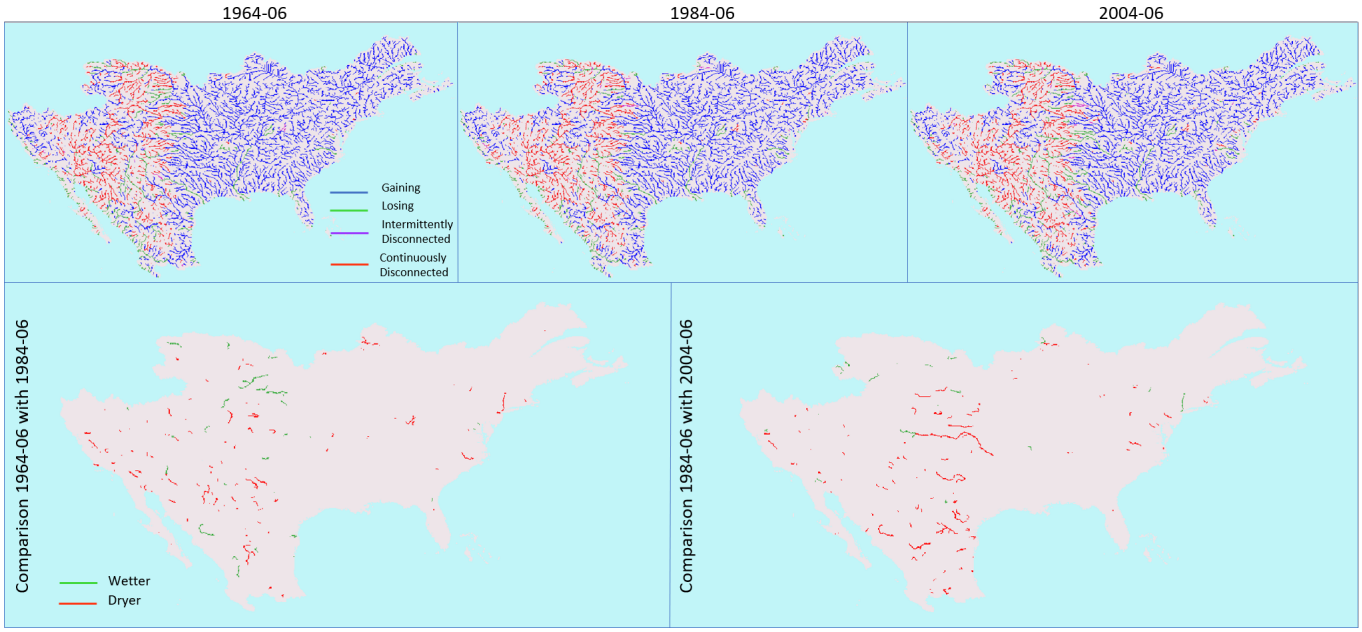

Figure C.4: Evolution of the states of streams over time for the reference run (historic + future) for first row: June 1964, June 1984 and June 2004. The second row shows changes to wetter (green) or drier(red) stream from June-1964 to June-1984 and from June-1984 to June-2004

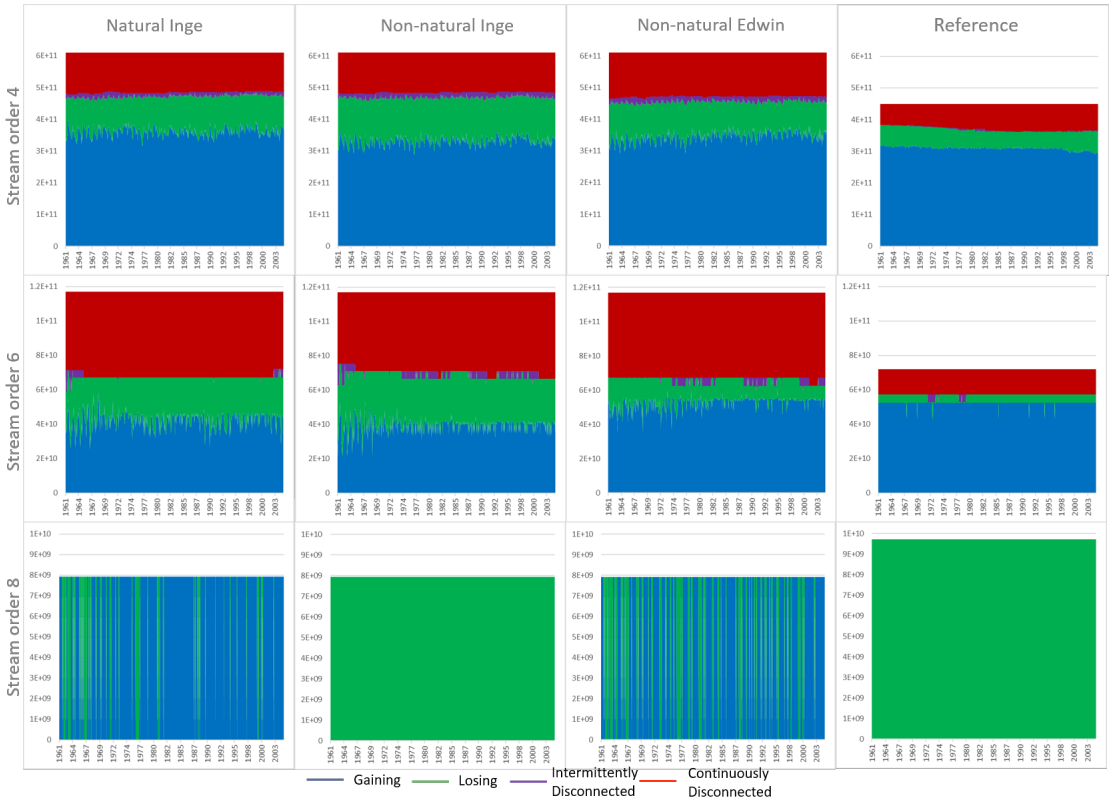

Figure C.5: Comparison in area (m2) between the change of state of stream for the different historic runs. The graph represent the cumulative area of stream of order 3, 5 and 7

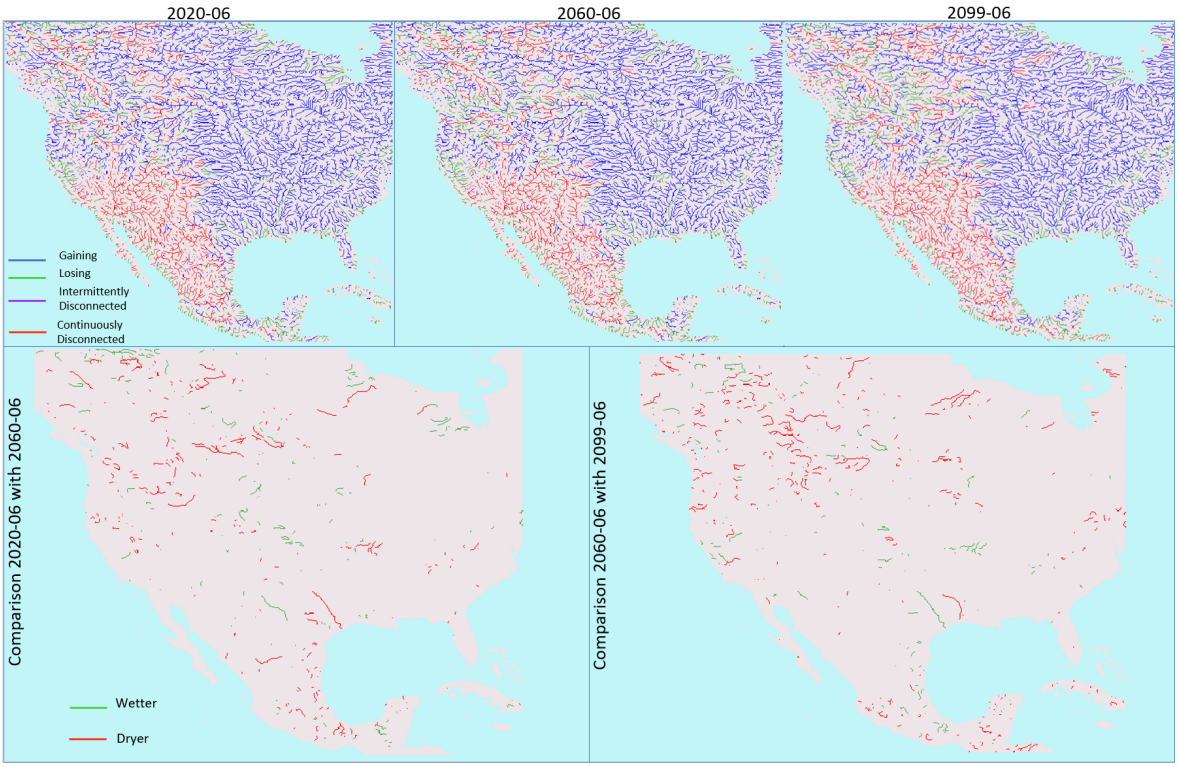

Figure C.6: Evolution of the states of streams over time for the HadGEM future non-natural run for first row: June 2020, June 2060 and June 2099. The second row shows changes to wetter (green) or drier(red) stream from June-2020 to June-2060 and from June-2060 to June-2099

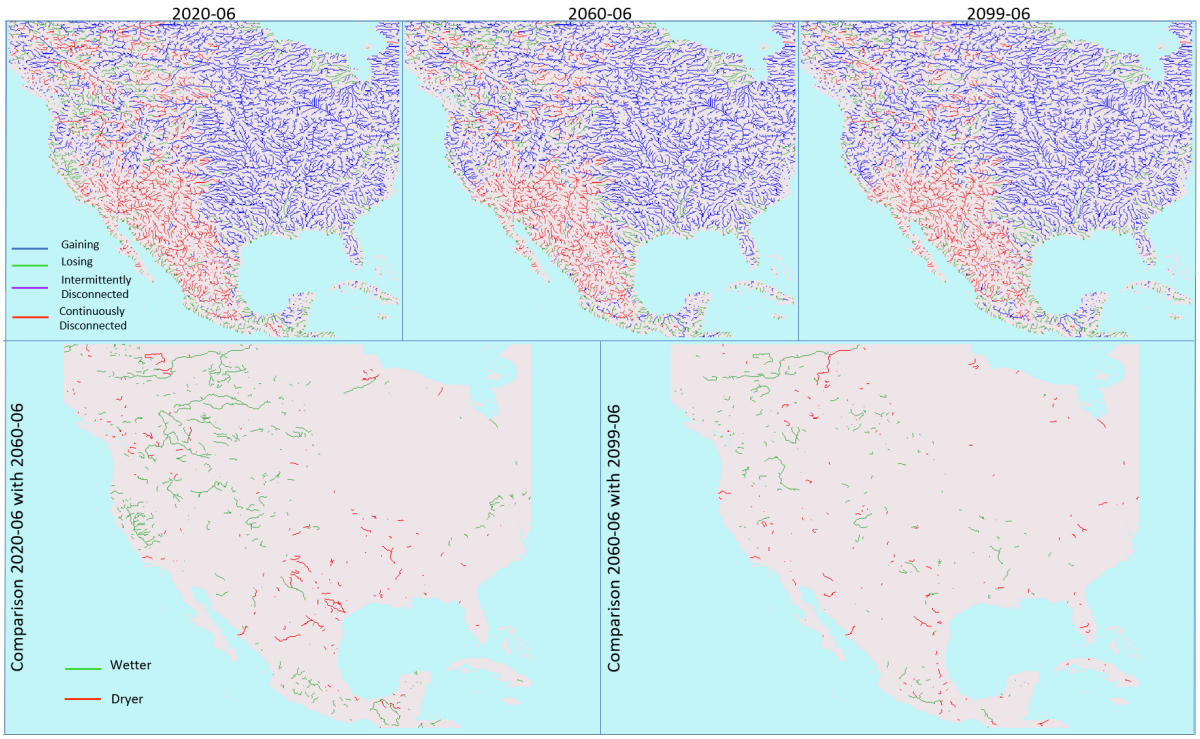

Figure C.7: Evolution of the states of streams over time for the GFDL future non-natural run for first row: June 2020, June 2060 and June 2099. The second row shows changes to wetter (green) or drier(red) stream from June-2020 to June-2060 and from June-2060 to June-2099

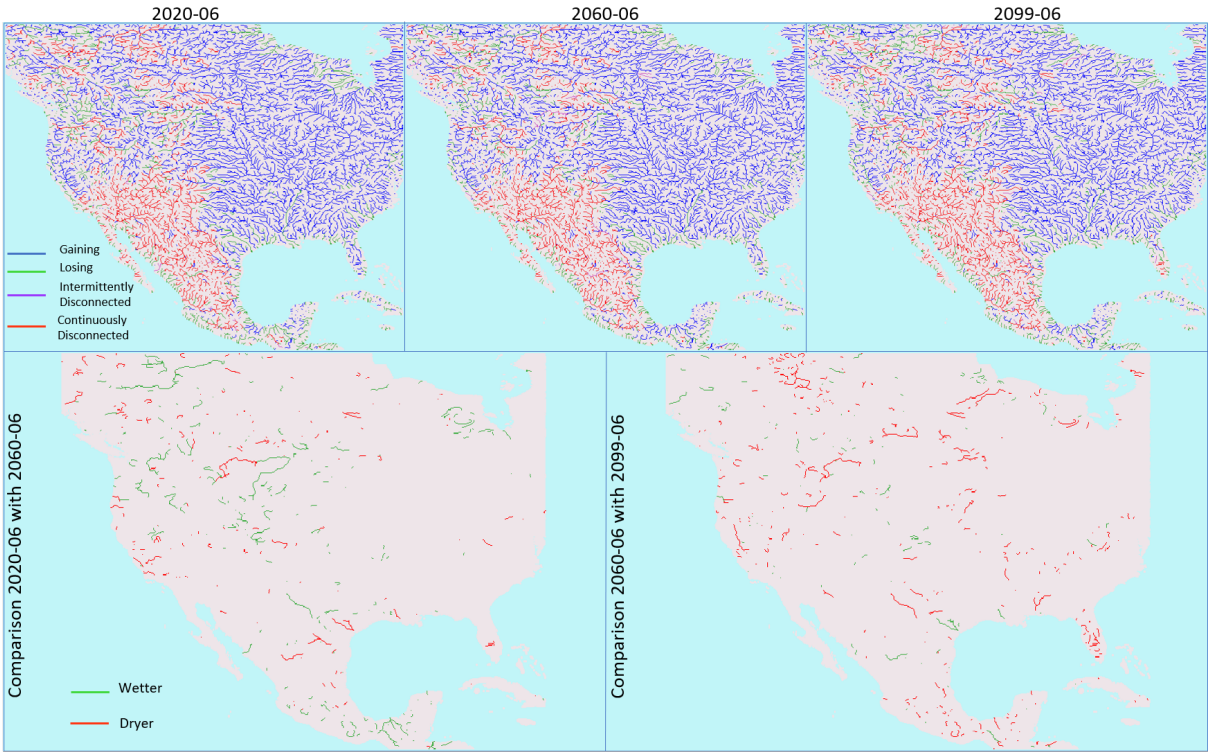

Figure C.8: Evolution of the states of streams over time for the MIROC future non-natural run for first row: June 2020, June 2060 and June 2099. The second row shows changes to wetter (green) or drier(red) stream from June-2020 to June-2060 and from June-2060 to June-2099

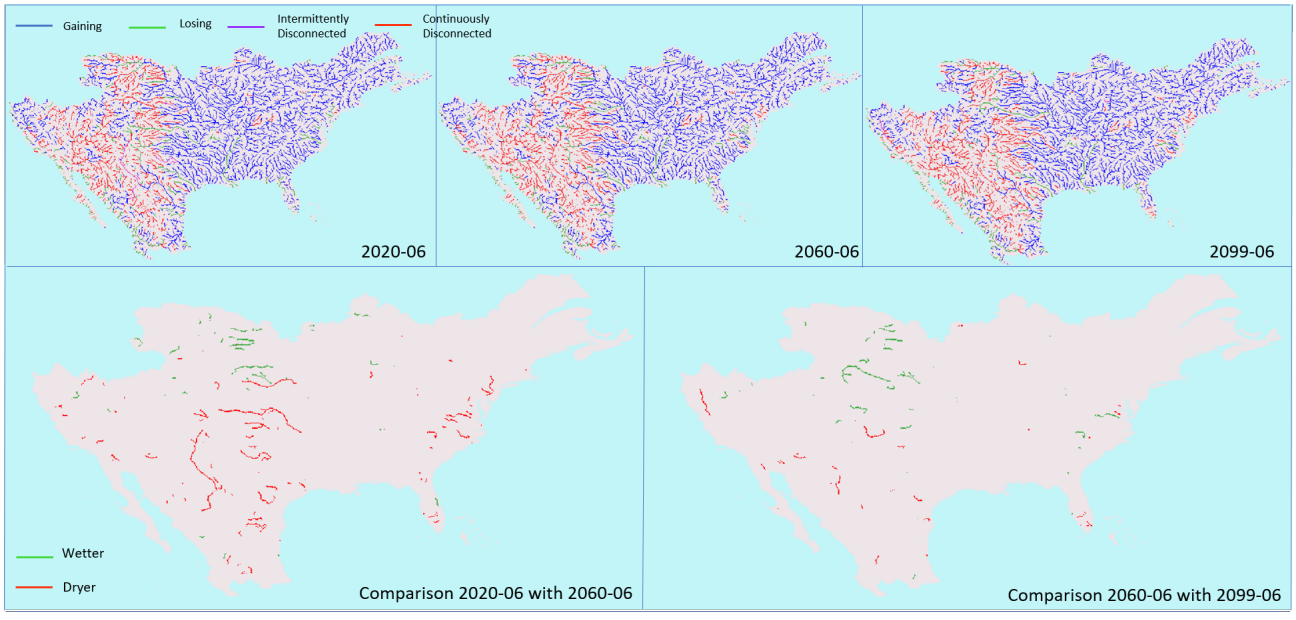

Figure C.9: Evolution of the states of streams over time for the reference run (historic + future) for first row: June 2020, June 2060 and June 2099. The second row shows changes to wetter (green) or drier(red) stream from June-2020 to June-2060 and from June-2060 to June-2099

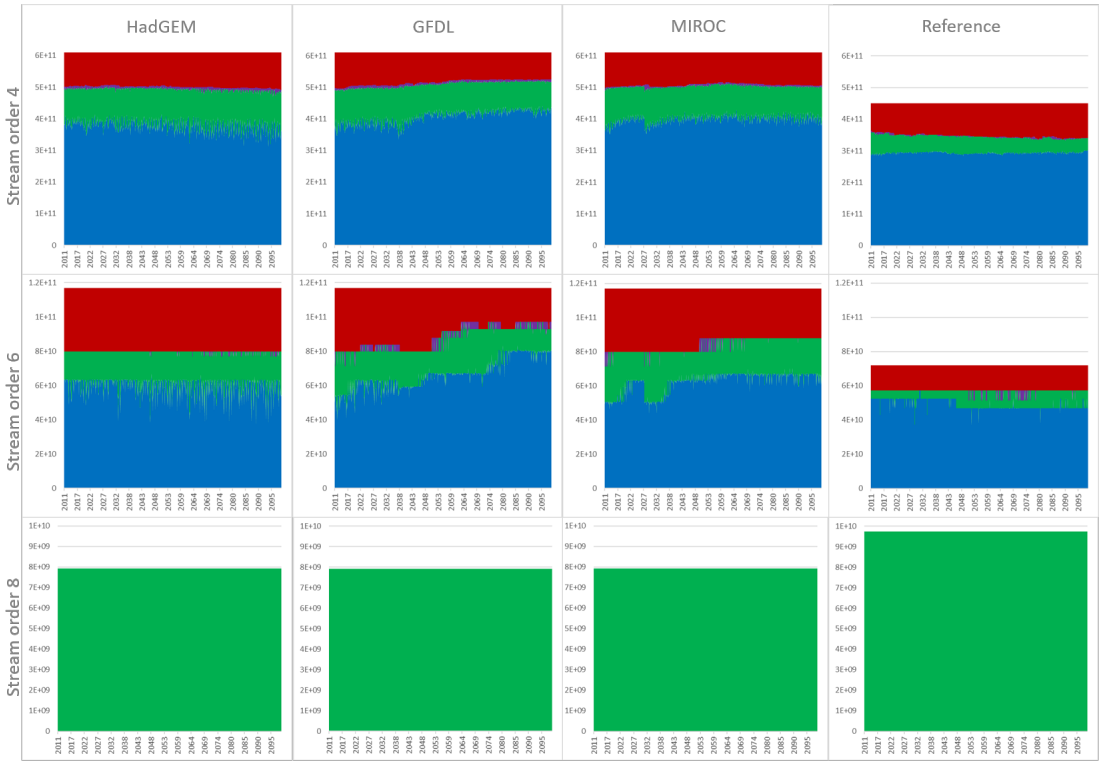

Figure C.10: Comparison in area (m2) between the change of state of stream for the different future runs. The graph represent the cumulative area of stream of order 3, 5 and 7

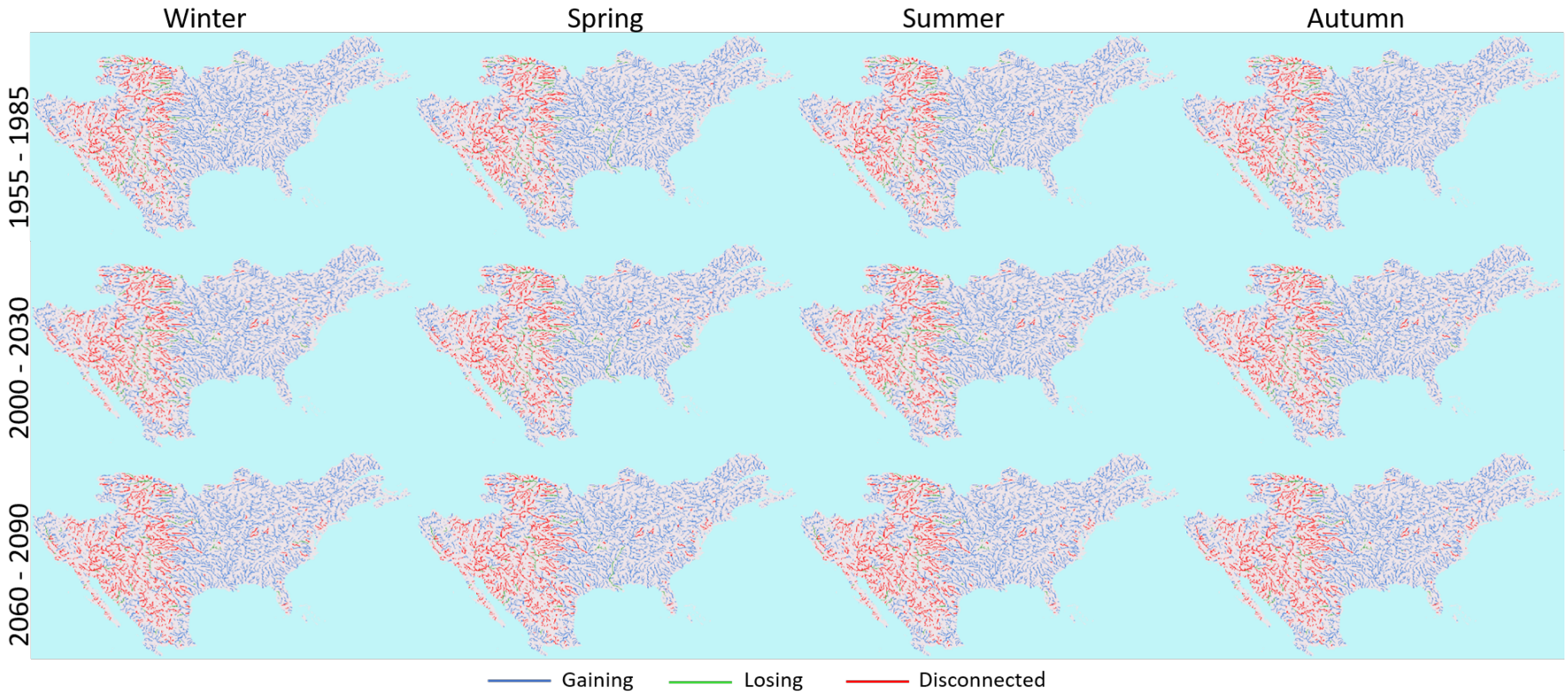

Figure C.11: Maps of a part of North-America showing the location and propagation/reduction of gaining, losing and disconnected streams for winter, spring, summer and autumn averaged on a period of 30-year. 1^{st} row: 1955-1985, 2^{nd} row: 2000-2030 and 3^{rd} row: 2060-2090.

D Important scripts

`final3map.py` Script

```
import numpy as np
import glob
import fileinput
import pprint
import string
import pandas as pd
import datetime
from dateutil.relativedelta import relativedelta
import itertools

dates = ['1950-01-28']
date1 = '19600131'  #start date
date2 = '20101231'  #end date
start = datetime.datetime.strptime(date1, '%Y%m%d')
end = datetime.datetime.strptime(date2, '%Y%m%d')
step= relativedelta(months=+1) # Delta of time is one month
fileOfDate = file("listOfDate.txt","w") #create a list of dates
while start <= end:
  print start.date()
  start += step
  result = str(start.date()) + '\n'
  fileOfDate.write(str(result))
fileOfDate.close()
dateList = open("listOfDate.txt").read().splitlines()
dates = list(itertools.chain(dates, dateList))
for i in range(len(dates)):
  dates[i] = str(dates[i]).replace('-28','')
  dates[i] = str(dates[i]).replace('-','')
print dates


# For the 'SO_type_interaction_stream_NA_*.asc' of every month look at all value that are the
    same
# for 24 month and if it is true, replace this value by 6
list_of_files = sorted(glob.glob('SO_type_interaction_stream_NA_*.asc'))
B=[]
B = np.fromstring(open(list_of_files[0]).read().replace('1e31','100'), dtype=int, sep=' ').
    tolist()
arrays = [B] * (len(list_of_files))
counters = [0] * (len(B))
last = arrays[0]
for j in range(len(list_of_files)):
    with open(list_of_files[j],'r') as FI:
    print j
    B = np.fromstring(FI.read().replace('1e31','100'), dtype=int, sep=' ').tolist()
    arrays[j] = B
    for i in range(len(B)):
      if counters[i] == -1:
        continue
      if B[i] == last[i]:
        counters[i] +=1
      else:
        last[i] = B[i]
        counters[i] = 0
      if counters[i] == 24:
        for j in range(i-24, i):
          B[i] = 6
      if counters[i] >= 24:
        B[i] = 6
#change the name of the file in order to add the year and month at the end
for i, j in zip(range(len(arrays)), dates):
  test = str(i) + '\t' +  str(j) + '\n'
  print test
  newIname= "replace2_SO_type_valueby6_{}.asc".format(j)
  print newIname
  afile=file(str(newIname),"w")
  for j in B:
    arrays[i][j] = B[i]
```

```
  arrays[i] = str(arrays[i]).replace(',',' ')
  arrays[i] = str(arrays[i]).replace('[',' ')
  arrays[i] = str(arrays[i]).replace(']',' ')
  afile.write(str(arrays[i]))
  afile.close()
```

allInOne_script_3dpart.sh Script

```
#!/bin/bash

#Change the asc file into a map file
for i in replace_SO_type_valueby6_*.asc;
do
echo $i
asc2map --clone ../../streamorder.map -S "$i" "${i%.asc}.map"
done

#If the value = 4 (continuously disconnected) in the SO_type_interaction_stream file replace it with the value in the replace_SO_type_valueby6
#file that can be only 4 or 6 if it was equal to 4 for at least 24 months
for i in SO_type_interaction_stream_*.map
do
 date=`echo "$i"|sed 's/\(SO_type_interaction_stream_\)\|\(.map\)//g'`
 echo $date
 pcrcalc "NB4interactionType_fin$date.map" = "if(SO_type_interaction_stream_$date.map==4, replace_SO_type_valueby6_$date.map,scalar(0))"
 pcrcalc "NB4interactionType_fin$date.map" = "if(NB4interactionType_fin$date.map==4,scalar(0), NB4interactionType_fin$date.map)"
 pcrcalc "Disconnected_continuus$date.map" = "scalar(NB4interactionType_fin$date.map) + scalar(SO_type_interaction_stream_$date.map)"
 rm "NB4interactionType_fin$date.map"
done

#change the map file into an asc file so that you can import it in excel
for i in Disconnected_continuus_*.map
do
 echo $i
 map2asc  "$i" "${i%.map}.asc"
done
```

area_count.py Script

```
import numpy as np
import glob
import fileinput
import codecs

#Set location and open file needed
with open('/scratch-shared/sophie/Natural_run/importantgraph/streamorder_maskNA.asc', 'r') as streamO:
  stremO= np.fromstring(streamO.read().replace('1e31','100'), dtype=int, sep=' ')
with open('/scratch-shared/sophie/Natural_run/importantgraph/cellsize05min_NA.asc', 'r') as cellarea :
  cellArea= np.fromstring(cellarea.read(), dtype = float, sep =' ')


#Apply on every file SO_type_interaction_stream_ and make a table with the area of gaining, losing, intermittently and continuously disconnected
list_of_files = sorted(glob.glob('finaltest_corr_Disconnected_continuus_*.asc'))
#need 'nothing" because value are respectively 1,2,3 and 4 , nothing are for values 0 that is not present in the map
names = ['nothing','losing','gaining','disconnect','c-disconnected']
Y=[None]*5
area_SO = open('area_SO_NA_gfdl_corr.txt', 'w')
for f in list_of_files:
    print(f)
    with open(f, 'r') as FI:
        B = np.fromstring(FI.read().replace('1e31','100'), dtype=int, sep=' ')
        print B.shape
        for i in range(5):
            Y[i]=[None]*6
            for j in range(6):
                k = j+3
```

```
                    I = np.where(B == i, stremO, 0)
                    #L = np.where(B==i, cellArea, 0)
                    Y[i][j] = np.where(I == k, cellArea, 0)
                    result = "{i}{j} = {val}".format(i=names[i],j=k,val=np.sum(Y[i][j]))
                    area_SO.write(str(f) +'\t'+ result +'\n')
                    print("{i}{j} = {val}".format(i=names[i],j=k,val=np.sum(Y[i][j])))
area_SO.close()
```